ON THE MECHANISM OF ACTION OF AN ION CHANNEL MIMIC

by
Katharine Clare Kaye
B.Sc., University of Victoria, 1988

A Thesis Submitted in Partial Fulfillment of the
Requirements for the Degree of

MASTER OF SCIENCE

in the Department of Chemistry

ACCEPTED
FACULTY OF GRADUATE STUDIES
[redacted]
DEAN
DATE 91/09/19

We accept this thesis as conforming
to the required standard

[redacted]
Dr. T.M. Fyles, Supervisor (Department of Chemistry)

[redacted]
Dr. D.A. Harrington, Departmental Member (Department of Chemistry)

[redacted]
Dr. R.A. Ring, Outside Member (Department of Biology)

[redacted]
Dr. W.W. Kay, External Examiner (Department of Biochemistry)

Supervisor: Dr. Thomas M. Fyles

ABSTRACT

The transport of alkali metal cations across the lipid bilayers of large unilamellar vesicles is mediated by a synthetic ion channel mimic, $(G8TrgP)_6$. The transport mechanism is determined by comparison to the behaviours of gramicidin D (an ion channel), and valinomycin (an ion carrier), in the same experimental system. The transport properties examined are concentration dependence, temperature dependence, cation selectivity and concentration dependence, and inhibition of the transport activity by octylammonium sulphate.

The concentration dependence of the mimic was examined over the range 0.008 - 0.154 mole percent of lipid. A similar set of experiments examined the behaviour of gramicidin over a concentration range of $(0.08 - 3.2) \times 10^{-3}$ mole percent of lipid, and for valinomycin, in the range of 0.017 - 0.17 mole percent of lipid. The results for the mimic showed a trend of increasing rate for increasing concentrations up to a saturation rate. This behaviour was observed for gramicidin, but not for valinomycin. Increasing concentrations of valinomycin increased the transport rates without reaching a saturation rate. Both the mimic and gramicidin were observed to have increasing extents of transport for increasing concentrations, but valinomycin had a constant extent of transport independent of its concentration.

The temperature dependence of all three transporters was investigated over the range 5 - 35 °C. The Arrhenius activation energies derived from the temperature dependence study were: $(G8TrgP)_6$ mimic, 16 ± 3 kJ/mol; gramicidin, 16 ± 2 kJ/mol; and valinomycin, 47 ± 7 kJ/mol. The difference between the activation energies of gramicidin and valinomycin is indicative of their different transport mechanisms. The activation energies of the mimic and gramicidin are identical, and on the order of thermal energies for the temperature range used

in this study.

The selectivity sequences were determined for the transporters by comparing rates and extents of transport for equal concentrations of the sulphate salts of lithium, sodium, potassium, rubidium, and cesium. The cation selectivity sequences for the transporters were all different: the mimic, $Cs^+ > Rb^+ > K^+ > Na^+ > Li^+$; valinomycin, $Cs^+ = K^+ = Rb^+ >>> Na^+ = Li^+ = 0$; and gramicidin had no apparent selectivity in this experimental system. The selectivity sequence of the mimic appears related to the size of the bare cation and/or the ease of dehydration of the cation. The sequence is not the same as for complexation to 18-crown-6 crown ether, nor is it the same as the sequence for the extraction of the cations into the lipid bilayer.

The dependence of rate of transport and extent of transport as a function of concentration of cesium and potassium cations was investigated. The Michaelis-Menton parameters, V_{max} and K_m, for transport of potassium were determined by a Lineweaver-Burk analysis. The parameters, for potassium transport, of V_{max} and K_m respectively, were: for the mimic, $0.19 \pm 0.03 \times 10^{-2}$ s^{-1} and 3 ± 0.2 mM potassium; for gramicidin, $0.30 \pm 0.09 \times 10^{-2}$ s^{-1} and 5 ± 0.4 mM potassium; and for valinomycin, $0.38 \pm 0.02 \times 10^{-2}$ s^{-1} and 34 ± 0.7 mM potassium. In general, the cation selectivity sequences and the Michaelis-Menton parameters were not indicative of transporter mechanism. It was observed that the mimic was capable of mediating the transport of magnesium and calcium cations.

The transport activity of the $(G8TrgP)_6$ mimic was inhibited in the presence of octylammonium sulphate. The inhibition of potassium transport was examined over the octylammonium concentration range of 0 - 230 times the concentration of mimic. At a 10:1 mole ratio of octylammonium cation to mimic, potassium transport was virtually blocked. At lower ratios, the rate of transport increased. Gramicidin activity was also inhibited with octylammonium sulphate. The activity of valinomycin was not affected.

In this experimental system, the $(G8TrgP)_6$ mimic had critical dissimilarities to the

behaviour of valinomycin, and insignificant differences compared to gramicidin. There were no similarities to valinomycin that could sustain an argument that the mimic acted with a carrier mechanism. The experiments produced strong evidence in support of the mechanism of the mimic being analogous to that of gramicidin.

Examiners:

[redacted]

Dr. T.M. Fyles, Supervisor (Department of Chemistry)

[redacted]

Dr. D.A. Harrington, Departmental Member (Department of Chemistry)

[redacted]

Dr. R.A. Ring, Outside Member (Department of Biology)

[redacted]

Dr. W.W. Kay, External Examiner (Department of Biochemistry)

TABLE OF CONTENTS

LIST OF TABLES

LIST OF FIGURES

ACKNOWLEDGEMENTS

I would like to express my gratitude to my supervisor, Dr. T. Fyles, for his help, encouragement, and guidance throughout this project. Many thanks to my co-workers, for their constant humour and support. Thanks to many other members of the Chemistry Department for their help and instruction, and to the support and secretarial staff, for their time spent on my many requests. I would also like to acknowledge the assistance of several members of the Biochemistry Department, and to acknowledge the efforts of Dr. Singla in helping me to use the Biology Department's Transmission Electron Microscope.

DEDICATION

To my husband and my son,

for keeping my perspective on

the important things in life.

INTRODUCTION

There is a substantial energy barrier to the translocation of alkali metal ions across a lipid bilayer - approximately 650 kJ/mol to move a sodium cation from water to the middle of a 30 Å thick membrane[1]. Facilitation of ion transport by lowering this energy barrier can be envisaged by two broad strategies: carrier or channel (see Figure 1). Both employ molecules which have polar sites to interact with the transported ions, the energy of complexation stabilizing the cation's exit from its aqueous environment, and a non-polar shell to interact with the lipid of the membrane. A *carrier* molecule resides in the membrane and diffuses freely from one face to the other. The carrier molecule extracts a cation from the aqueous solution by exposing its polar sites at the membrane aqueous interface and complexing the ion. Once complexed the ion is within a polar core, enveloped by a non-polar shell. The complex diffuses to the other side of the bilayer, and the ion is released. A *channel* molecule remains stationary within the membrane, and both its polar core and lipophilic shell must span the bilayer. A cation could enter the channel by complexation to the polar sites, or by simple diffusion into the lumen of the structure. In essence, the channel structure provides a hole through which ions may travel across the membrane. In either case, ion transport is facilitated because the cation is continuously in a polar environment.

Naturally occurring carrier molecules form the necessary inclusion complexes of cations. Some typical examples of these molecules are valinomycin[2], nigericin[3], and monensin[4] (see Figure 2). In the process of evolution, these molecules apparently[5] were developed by microorganisms as a defence mechanism. The macrocycle valinomycin collapses any potassium gradient across a cell membrane, thus reducing the potential energy which makes the production of adenosine triphosphate in a cell possible; without ATP, a cell that was attacked by valinomycin, dies[5]. Nigericin and monensin are acyclic ionophores which form pseudo-cyclic inclusion cation complexes by head-to-tail hydrogen bonding[6]. Of course, discovery of these molecules and their transport activity in membranes lead to the synthesis of carrier mimics;

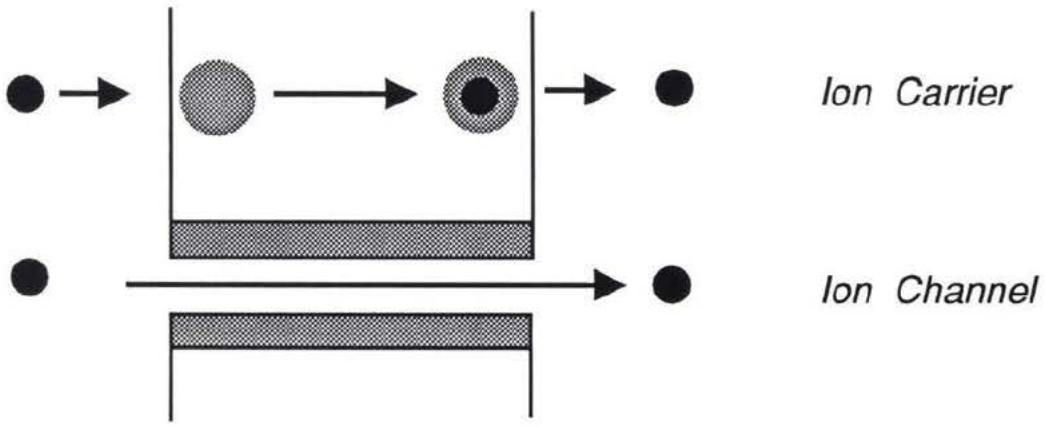

Figure 1 Schematic Mechanisms of Two Strategies for Ion Transporters

for example, cyclic octapeptides[7], analogues of 1,2-ethylenedioxydiacetic acid[8], and mimics of nactins and valinomycin[9] themselves. A review by Fyles[9] summarizes the biomimetic carrier literature to 1988; at that time there were several hundred synthetic carrier molecules reported. A recent review by Tsukube[10], in addition to covering the list of new carrier mimics, also sets out the design strategies for cation and anion transport. Since carriers work via diffusion the membrane thickness is irrelevant to their function, thus they can be studied easily in liquid membrane systems. Carriers are also studied in lipid bilayer systems, and it has been observed that their behaviours can differ between the two membrane systems[6]. The studies comprise determinations of activation energies, absolute rates of transport, cation selectivities, kinetic order, and structural variation.

The foremost natural channel forming molecules are proteins, comprised of large and complex polypeptides, folded to span a cell membrane. The majority of these proteins utilize α-helices to organize the amino-acid units into an ion channel structure, where the polar side

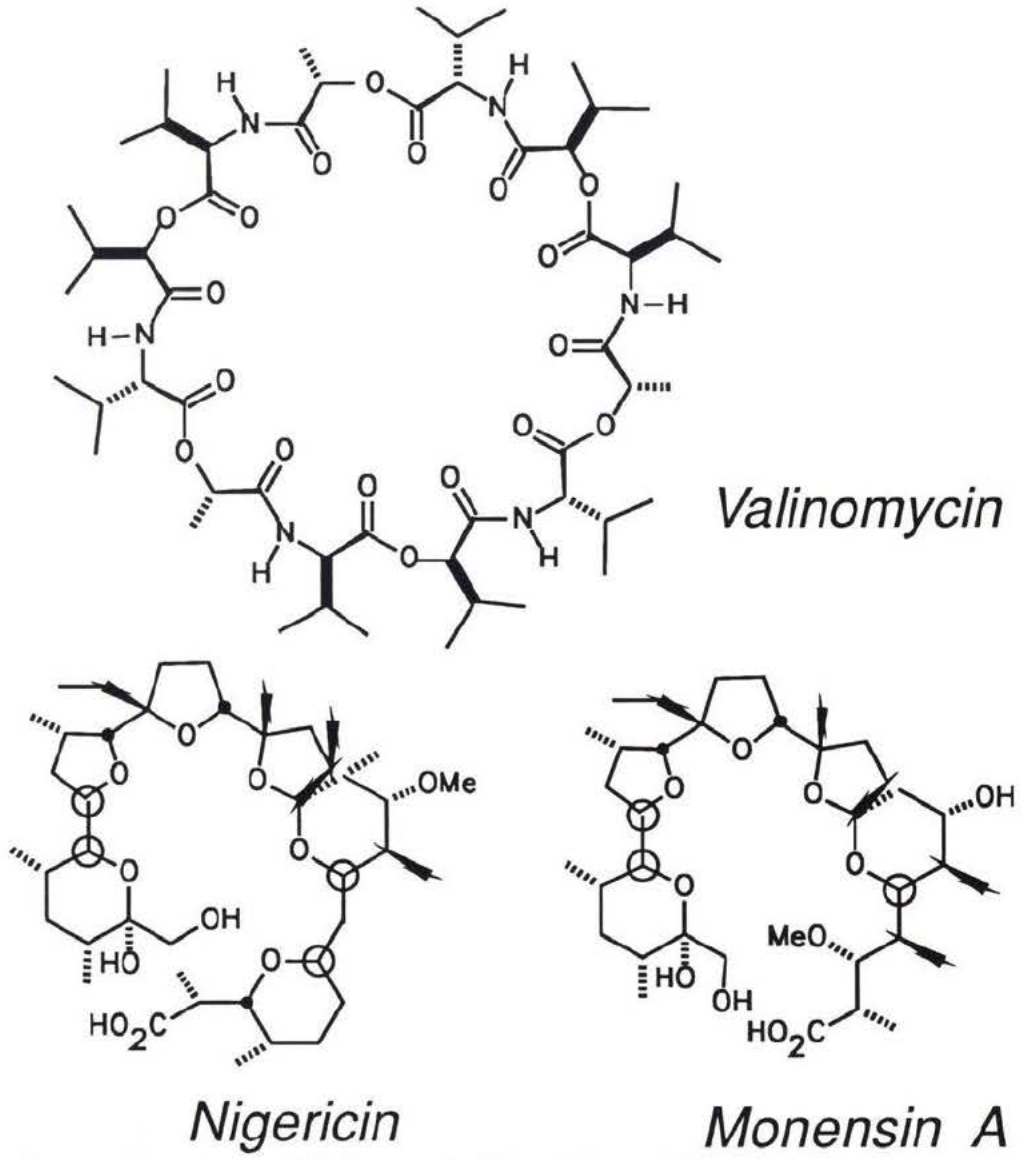

Figure 2 Structures of Valinomycin, Nigericin, and Monensin

chains form the polar core of the channel, and the non-polar side chains become the lipophilic shell. For example, bacteriorhodopsin comprises up to 50% of the membrane of the bacterium, *Halobacterium halobium*. The bacteriorhodopsin protein contains seven α-helical segments, some of which form the channel structure for the pumping of protons across the membrane wall to create a gradient which will drive the bacterium's metabolic processes[11]. Another example, the acetylcholine receptor protein is involved in cell-cell communication[12]; it responds to the binding of acetylcholine by momentarily opening and allowing the passage of only selected cations. The channel structure consists of four helical subunits which span the membrane[13]. Even with the vast amount of research into these and other biologically active

channels, determination of the precise transport pathway through any channel structure has been unsuccessful. High resolution of the structures are not known, therefore the molecular details of the ion translocation process are not known.

There are simpler polypeptide molecules which also are capable of ion transport, such as gramicidin (see below), alamethicin[14] and melittin[15]. Alamethicin can form cation selective, voltage gated channel structures through aggregation of several helical monomer units[16]. Melittin aggregates to form a tetramer channel structure in membranes and causes apparent lysis of the bilayer[16]. Mimics of these compounds are based on forming helical structures through synthesis of simple polypeptide chains. De Santis[17] *et al.* showed that poly(DL-proline) behaved in BLM conductance studies similarly to gramicidin A. The cation selectivities were different, due to the difference in the lumen diameters[17]. Kono *et al.*[18] have recently shown that an amphiphilic polypeptide, poly(lysine - 2-aminoisobutyric acid - leucine - 2-aminoisobutyric acid), is conformationally dependent on pH. It can mediate the release of NaCl from polyamide capsules when used as an additive to a membrane coated on these capsules. Spach *et al.*[19] also have synthesized a polypeptide monomer which folds into an α-helix and aggregates into a channel forming structure. Pullman[20] has written a brief summary on the study of synthesis of polypeptide helices for the formation of channel structures. Generally, polypeptide mimics have shown activity and possible utility, but the factors controlling their behaviour have not been systematically investigated.

There are also a few non-peptide mimics which have been successfully synthesized (see Figure 3). Tabushi *et al.*[21] have synthesized a "half channel" by attaching long hydrocarbon arms onto β-cyclodextrin, which apparently transported copper (II) and cobalt (II) across artificial liposomes. Gokel *et al.*[22] have synthesized a string of three crown ethers, joined by hydrocarbon chains, which was postulated to stack within a lipid bilayer, thus forming a relay of complexing sites across a membrane. The initial experiments showed that this "tris(macrocycle)" facilitated transport of sodium across vesicle walls, a channel mechanism

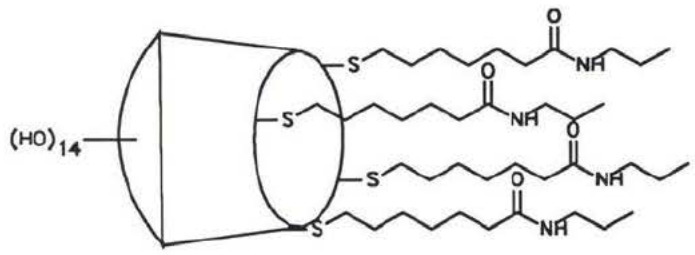

Tabushi - "half channel"

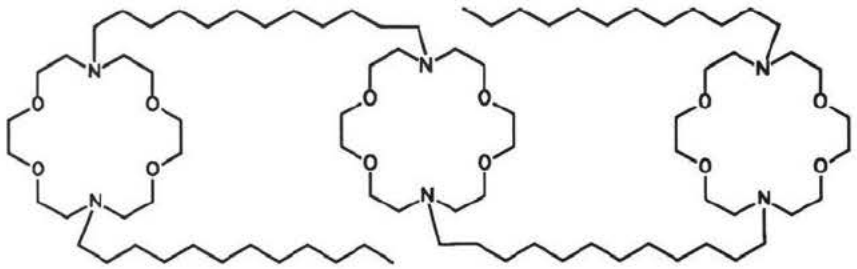

Gokel - "tris(macrocycle)"

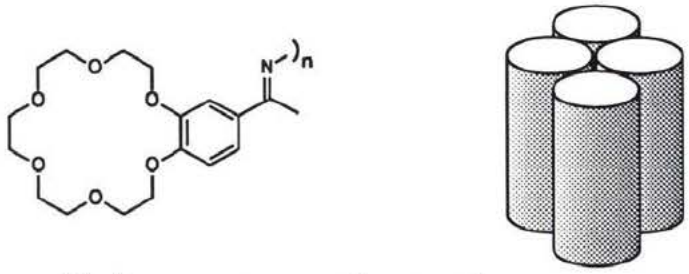

Nolte - crown ether polymer

Figure 3 Schematic Representations of the Mimics of Tabushi, Gokel, and Nolte

was proposed. Menger *et al.*[23] found that polyether intermediates in the synthesis of a potential "flux-promoting" compound were capable of ion transport. Sadly, the goal of the synthesis was not active. Structural variation of the intermediates produced compounds which displayed greater activity than gramicidin in the assay system used. Nolte *et al.*[24] polymerized crown ethers into high molecular weight channel-forming structures. Transport experiments were done to monitor the loss of cobalt from the exterior of vesicles containing the polymer, and the gain of cobalt within the vesicles. The results clearly identify the polymer as capable of facilitating transport of cobalt (II) across bilayers; some of the evidence presented points to

a channel mechanism. Fyles *et al.*[25] synthesized a channel mimic by attaching macrocyles to both faces of a crown ether framework, and glucose derivatives onto these macrocyclic arms. This mimic was shown, by monitoring fluorescein trapped in vesicles, to promote the translocation of sodium cations across lipid bilayers. Further study[26] showed the mimic to have many similarities to the behaviour of gramicidin. Lehn *et al.*[27] have suggested approaches (as yet non-functional) to mimics based on crown ether frameworks: a "trimeric stack" of crown ethers, and a "chundle" incorporating branching hydrocarbon arms in place of the macrocyclic arms of the Fyles[25] approach. At this time there are several different non-peptide channel mimics; some are reasonably well characterized but the mechanistic studies to date are very limited.

The best studied and least ambiguous channel forming molecule is gramicidin A. It is a linear pentadecapeptide of alternating D- and L- chirality, which takes on a left-handed β-helix configuration (or Π^6 helix) in bilayers. The gramicidin channel is formed by head-to-head dimerization at the amino termini (see Figure 4). It has been studied extensively due to its

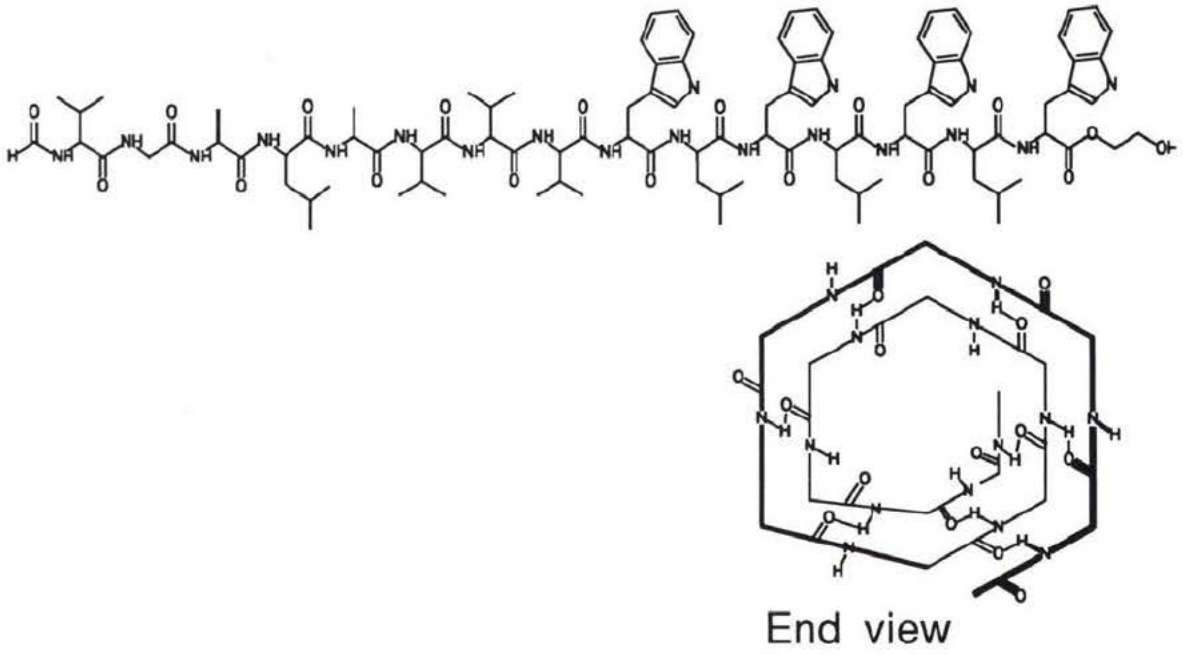

Figure 4 The Structure and Schematic Organization of Gramicidin

structural simplicity, and ready availability. It is very well characterized in black lipid[28] and vesicle membranes[2], and is frequently reviewed[1,28,29,30] as a general model for biological ion channels. The dimer forms a 26 Å long, 4 Å wide orifice through the bilayer, and selectively transports rubidium and cesium cations over potassium, sodium, and lithium (in descending order of permeability[1]). The sequence of binding sites, and their respective affinities for each of the cations, has been documented[31]. Conductance studies in BLMs show a step-function of current versus time, indicative of a channel mechanism. In essence, gramicidin defines the concept of a "channel".

With respect to carriers, valinomycin (see Figure 2) has been studied in depth as well. It is a cyclododecadepsipeptide (alternating hydroxy- and amino- acid groups) which forms a "...bracelet 9.4 Å high and 16.4 Å in diameter..."[32] capable of complexing rubidium, potassium, and cesium very well[33] and transporting them across lipid bilayers. Valinomycin is capable of a slow antiport of cations and protons, but the transport rates are substantially increased in the presence of a proton gradient decoupler such as carbonyl cyanide-p-trifluoromethoxy-phenyl hydrazone (FCCP)[34]. Although less central than gramicidin, valinomycin serves to define the concept of a "carrier".

Schematically, it is simple to visualize the difference between carriers and channels: a channel is large enough to span a bilayer and is stationary in that bilayer compared to a smaller and mobile carrier. Unfortunately, the kinetic and thermodynamic differences between the two mechanisms are difficult to define and the criteria for establishing a potential mimic as having a carrier or channel mechanism are limited. The most direct method of determining the mechanism of a transporter is through bilayer membrane conductivity experiments (see Figure 5). In these experiments, a small planar bilayer is formed on the end of a capillary electrode. The transporter is incorporated into the bilayer before or after membrane formation. An electrical potential is applied across the membrane and the function of current versus time, the result of ions transported through the bilayer, is indicative of the transporter mechanism.

A channel mechanism produces a step-function due to the all or nothing, open or closed states of the molecule. Carriers do not exhibit discontinuities in current amplitude and give only a general increase in conductivity. In place of these membrane conductance measurements, other less rigid guidelines have been proposed, two of which follow.

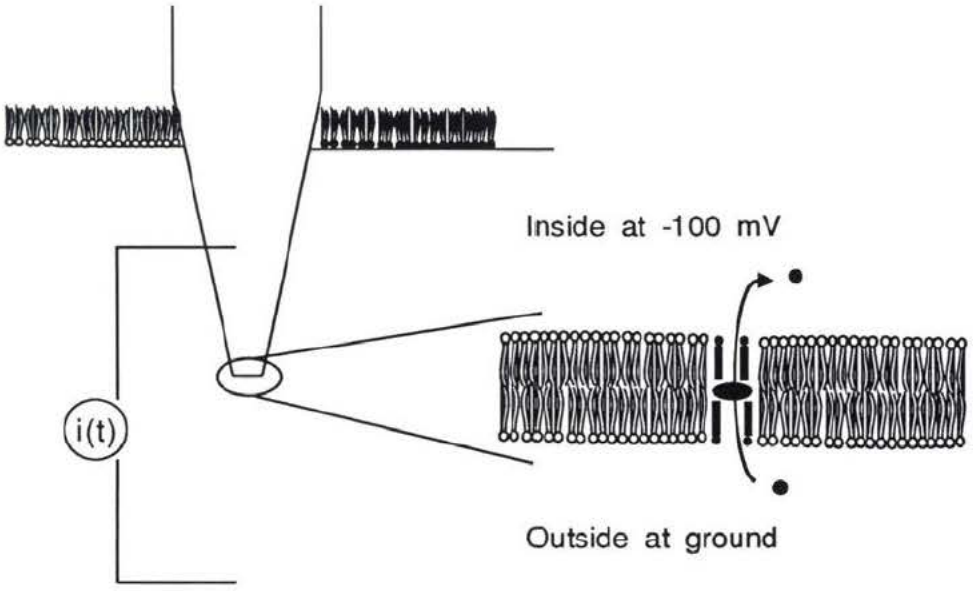

Figure 5 Schematic of the Membrane Conductivity Experiment Using the Pipette-Dipping Technique

One guideline was proposed by Eisenman *et al.*[36] who compared valinomycin and gramicidin transport rates in the crystalline and gel phases of a black lipid membrane. The results implied that valinomycin does not function in the crystalline state. On the other hand, gramicidin does function and does have a temperature dependence below the phase transition. In the gel phase, valinomycin had a temperature dependence and gramicidin did not. The activation energy of gramicidin was so low that ion transport was essentially unaffected by temperature. The general conclusion was that carriers do not function in the crystalline phase, but channels do.

Another guideline was proposed by Gary-Bobo *et al.*[2] who also compared valinomycin to gramicidin. In studying the effect of increasing concentration on the observed transport rates, it was observed that the extent of transport was constant and independent of valinomycin

concentration. Conversely, the extent of transport was dependent on gramicidin concentration. This reflects the "all or nothing" mode of action of a channel, such that a single opening event per vesicle is capable of collapsing the cross-membrane gradients of that vesicle. The transport of about 10^5 ions would be sufficient. Once the channel has collapsed the gradients it apparently remains in the vesicle. Carriers, functioning by diffusion, have comparatively slower rates, but are able to move in and out of several vesicles, thus eventually collapsing all gradients in the system.

There are two choices for the system in which to analyse a potential biomimetic channel: planar bilayers such as black lipid membranes (BLMs) or the pipette-dipping technique of Figure 5, or vesicles. BLMs are used quite frequently to characterize transporters.[19,17,35,36] Black lipid membranes are usually formed across a pinhole separating two aqueous compartments by applying a drop of lipid/solvent over the hole. The drop thins and a planar bilayer eventually forms in the center of the hole, surrounded by a torus of solvent. Vesicles are spherical, cell-like structures composed of one or more bilayers, of any number of lipids, which surround, and are surrounded by, water[37]. They can be small (100 Å) or large (5000 Å), and uni- or multilamellar. Vesicles are more like the bilayer component of cell structures, and can provide a reasonable system in which to analyse a transport mimic.

In any study utilizing vesicles, heterogeneity of the prepared vesicles is a problem. Multilamellar vesicles are the easiest to make since the addition of water to lipid results in their spontaneous formation[38]. However, the number of bilayers within multilamellar vesicles varies greatly and cannot be controlled. More importantly, the entrapped volume is very low. Small unilamellar vesicles are fairly easy to make - sufficient sonication of a multilamellar suspension will break down the water-in-oil droplets to a minimum size[38]. These vesicles also have a very small entrapped volume. Large unilamellar vesicles require much more effort to prepare[39], but have a large entrapped volume. Their size distribution can be controlled with filtration[39] through polycarbonate filters.

Vesicle studies use the impermeability of the membrane to maintain set pH and ion gradients between the inner and outer aqueous solutions. Addition of a transporter to the membrane collapses these gradients to differing degrees and with differing rates depending upon the transporter and cation used. The common methods of monitoring the collapse of pH and cation gradients are NMR, fluorescence or UV/VIS absorption, and pH-stat titration. The studies using NMR monitor either the translocation of a spin active cation, or the relaxation and change in chemical shift of the phosphate headgroup populations on the inside and outside of the vesicle wall. Typical NMR[22] studies require high concentrations of vesicles, and hence large amounts of transporter which is not always feasible. Fluorescence[40,42] studies utilize

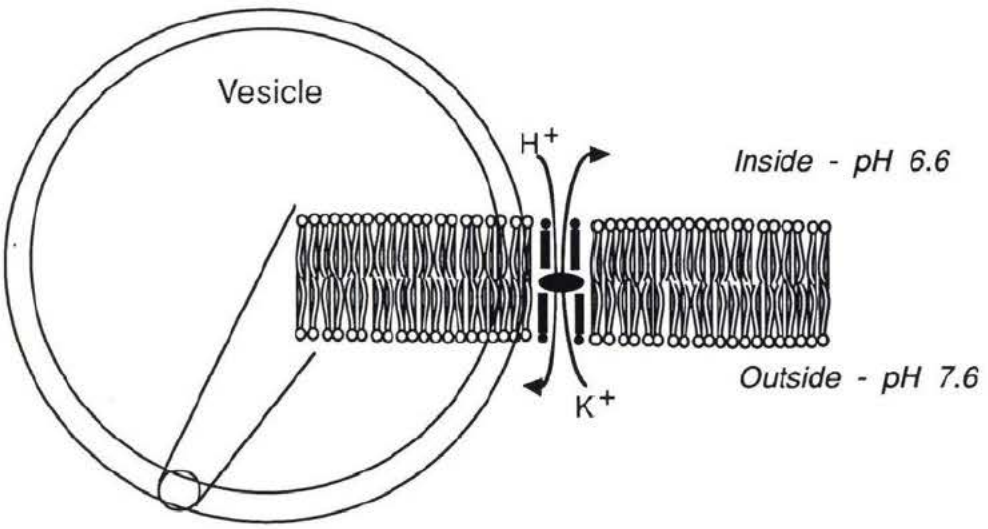

Figure 6 Schematic of Cation and Proton Antiport through an Ion Channel in a pH-stat Experiment

either an entrapped dye or a derivatized lipid which is fluorescent in a closely packed system (i.e. does not self-quench). This method, and similarly the UV/VIS absorption method[24], requires sufficient concentrations of a pH or cation concentration dependent dye to actually monitor, and large enough gradients across the membrane that the collapse is detectable. The pH-stat titration method is an indirect way to examine the movement of ions across cell walls (see Figure 6). The collapse of the cation gradient across the vesicle membrane is coupled to

a proton antiport, thus involving a change in pH in the bulk "outer" solution. Titration to maintain a set pH in the bulk solution while the transport is occurring reports the rates of the transport event. All that is required is sufficient entrapped volume that the collapse of the pH gradient can be detected.

The synthesis of the precursor of the transporter mimic studied in this report was completed by Vicki Carmichael, Philip Dutton, and Jennifer Swan at the University of Victoria[25]. In a preliminary survey Dutton and his colleague Tony James showed that the molecule did indeed facilitate the translocation of potassium ions across vesicle membranes[25]. Further studies[26] showed a cation selectivity, and several other properties which indicated that Dutton's molecule had a mechanism similar to gramicidin. James then synthesized numerous analogues, producing better characterized molecules of higher purity with respect to stereochemistry and complete functionalization. The channel mimic for this study was synthesized by James and is pictured in Figure 7. The crown ether core was synthesized from tartaric acid units to create a hexa-acid 18-crown-6 macrocycle. The stereochemistry dictated

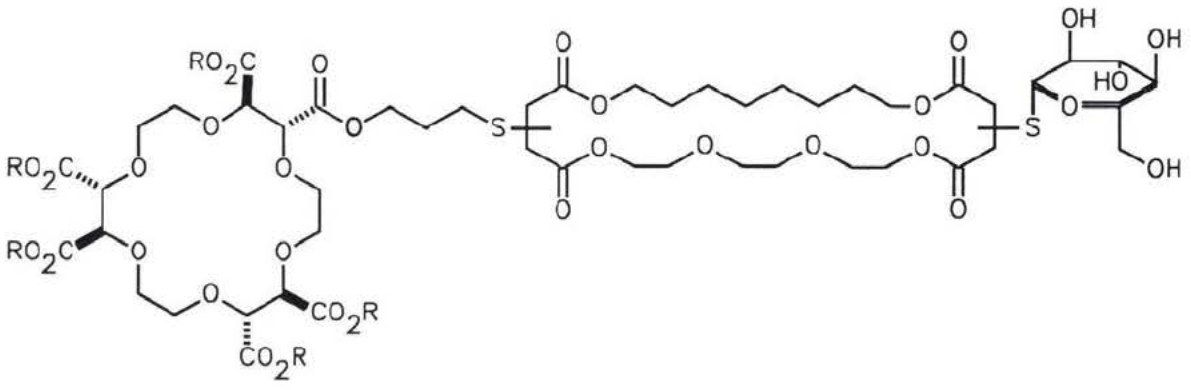

Figure 7 Structure of the $(G8TrgP)_6$ Mimic Synthesized by James

that the six carboxylic groups would alternately orient on the opposite faces of the crown. Six

macrocyclic arms were attached to the crown ether via carboxylic esters to form the walls of the channel. These macrocycles provided different polarities in the walls to mimic the polar-inside/ lipophilic-outside characteristics of the natural channel molecules. For synthetic reasons a short alkyl spacer was attached to the macrocycle to link to the hexa-acid crown framework. In the Dutton mimic, the spacer was 2-thioethanol; James used 3-thiopropanol. The difference between the use of these linkages was compelled by the addition chemistry of the macrocycle to the crown. Dutton formed the ester via an acid chloride; James used the carboxylate to displace a leaving group on the spacer unit. After the addition of the arms to the crown, β-1-mercapto-D-glucose was added to ends of the arms to act as headgroups capable of interacting with the headgroups of membrane lipids and with the surrounding water.

The IUPAC name for this compound is long: hexakis[(3- and/or 4-(17- and/or 18-(β-D-glucopyranosylthio))-1,6,9,12,15,20-hexaoxa-2,5,16,19-tetraoxocycloctacosyl)-4-thiabutyl))] (2R,3R,8R,9R,14R,15R)-1,4,7,10,13,16-hexaoxacyclooctadecane-2,3,8,9,14,15-hexacarboxylate; the abbreviated version is much simpler: $(G8TrgP)_6$. The abbreviation describes the channel with respect to its functional parts: G stands for the glucose headgroup; 8 describes the number of methylene units on the lipophilic side of the arms; Trg is an abbreviation for the triethylene glycol chain incorporated into the polar side of the arms; P describes the length of the hydrocarbon chain linking the arms to the crown, in this case a propyl group; and $_6$ is the number of arms on the crown core[41].

This thesis reports the results of pH-stat experiments used to examine temperature and concentration dependence, cation selectivity and concentration dependence, and inhibition of activity of the $(G8TrgP)_6$ mimic. Also mentioned are the results of planar membrane conductivity experiments performed by Dr. Mark Sansom of Nottingham University, England. The first goal of a detailed examination of the mimic was to show that it was actually a transporter. Did it facilitate the translocation of ions through the vesicle membrane without acting as a detergent, without forming defects in the membrane, and without creating large

water-filled holes which allow passive diffusion of ions? The mimic is presumed to act by either a carrier or a channel mechanism. The subsequent phase of this study sought to establish which mode of action applied in this case. Since the study utilizes vesicles as the membrane system then only indirect study of the mimic's actions is possible. Therefore, the decision with respect to the transporter mechanism of the mimic can only be made upon pairwise comparison of the mimic to valinomycin and gramicidin, known to act as carrier and channel, respectively.

EXPERIMENTAL

General Instruments

The titration system was a Metrohm 655 Dosimat buret and titration cell, 614 Impulsomat automatic titrator, and 632 pH-meter. The buret was linked to an HP-85 microcomputer for data acquisition. Vesicle preparation required use of a Heat Systems W385 Ultrasonic sonicator, located in the University of Victoria's Biochemistry and Microbiology Departments. Size distribution analysis of vesicles was performed using a Philips EM360 Transmission Electron Microscope, located in the Biology Department, and the Perkin-Elmer Model Lambda 4B Ultraviolet/Visible Spectrophotometer, in the Chemistry Department.

Vesicle Preparation

Egg phosphatidylcholine and egg phosphatidic acid (egg PC and PA) were purchased from Avanti Polar Lipids, Inc., Pelham, Alabama. Cholesterol was purchased from Sigma/Aldrich. Anhydrous diethyl ether and HPLC grade chloroform were purchased from BDH; methanol, choline hydroxide (20% in water), D-mannitol, and Bis-Tris (2,2-bis(hydroxymethyl)-2,2',2"-nitrilotriethanol) from Sigma/Aldrich; sulphuric acid (ultrapure) from Fluka; and PD-10 Sephadex G-25M columns from Pharmacia. Only D^3 (deionized, double distilled) water was used.

Stock Solutions

Choline Sulphate - Choline hydroxide (250 mL of 20% solution) was titrated to pH 6.5 with concentrated sulphuric acid. Activated charcoal was added, and the solution stirred for 10 minutes; the charcoal was removed by filtration through Celite, and the solution concentrated by rotary evaporation. One half liter of 100% ethanol was added and the tarry residue was dissolved with heating. Anhydrous ether (200 mL) was added and the solution cooled to -10 °C for 16 hours; the crystalline precipitate was removed by filtration. The mother liquor was returned to the freezer for overnight to yield a final crop of precipitate. The combined batches of choline sulphate precipitate were dried for 24 hours by vacuum.

Internal Buffer Solution - 0.20 M bis-tris, and 0.054 M D-mannitol; the pH was adjusted to 6.60 using 0.45 M H_2SO_4. Internal buffer was made in 500 mL batches.

External Solution - 0.110 M choline sulphate, and 0.093 M D-mannitol; made in one liter batches, portioned into 200 mL glass bottles and kept refrigerated as much as possible. Filtration through Millipore GS 0.22 μm filters extended the life of external solution.

Choline Hydroxide Titrant - one liter of 4.75 mM choline hydroxide, and 0.35 M D-mannitol, dissolved in D^3 water that was boiled for 30 minutes to release carbon dioxide. This solution was made in a nitrogen filled glove bag to avoid carbon dioxide contamination. The base titer was established by titration versus standard potassium hydrogen phthalate.

Egg Lecithin Vesicle Preparation

The egg lecithin vesicles were made by reverse evaporation[39], followed by sizing filtration and size exclusion chromatography. Each batch generated vesicles for approximately 16 pH-stat experiments. The following prescriptive procedure yields the most reproducible and reliable batches of vesicles for pH-stat work; that is, most of the entrapped buffer is within large unilamellar vesicles.

The vesicle bilayer composition is an 8:1:1 molar ratio of the egg PC and PA and cholesterol (or a 16:2:1 weight ratio). Make a chloroform stock solution of the 8:1:1 mixture, at a concentration of 50 mg PC per 6 mL; this limits the lipids' exposure to air, and simplifies the vesicle making procedure. Store under nitrogen in the refrigerator (0 - 5 °C); do not leave the solution at room temperature more than 5 minutes at a time.

Transfer 6 mL (50 mg PC) of the lipid/cholesterol solution to a 50 mL round-bottom flask, and immediately evaporate to dryness on a rotary evaporator. Remove all traces of chloroform from the lipid film by drying under vacuum overnight at ambient temperature, or for four hours with the flask in a 50 °C water bath. After the film is completely dry, add 6 mL of anhydrous diethyl ether to the flask, and quickly dissolve the dried lipid film. Add 2 mL of internal buffer. Stopper the flask with a nitrogen filled balloon to reduce the lipids' exposure

to air.

Sonication of the lipid/ether/buffer solution mixes this "water in oil" mixture to homogeneity. Once the sonicator is tuned (13 mm tip), apply 2 second pulses (at 50 % duty cycle and 5 power output) until the mixture is translucent gray. Stopper the flask with the nitrogen balloon. Reverse evaporation of the solution yields mostly large unilamellar vesicles with a high percentage of buffer entrapment. Remove the ether from the mixture by slow rotary evaporation, warming the flask with a 25 °C water bath. As the ether begins to evaporate, the solution coats the sides of the flask; further evaporation promotes spontaneous bubbling. This bubbling continues for about 5 minutes, until almost all the ether has evaporated; the system goes through a gelatinous phase, then becomes a liquid. Add 3 mL of the external buffer, and continue rotary evaporation for half an hour at a slightly reduced vacuum.

The filtration unit sizes the vesicles by forcing the vesicle solution first through a 1 µm Nucleopore filter, then a 0.4 µm filter (see Figure 8). Using a 16 gauge 10 mL disposable syringe collect the vesicle solution, draw a further 2 mL of air, and inject the vesicle solution

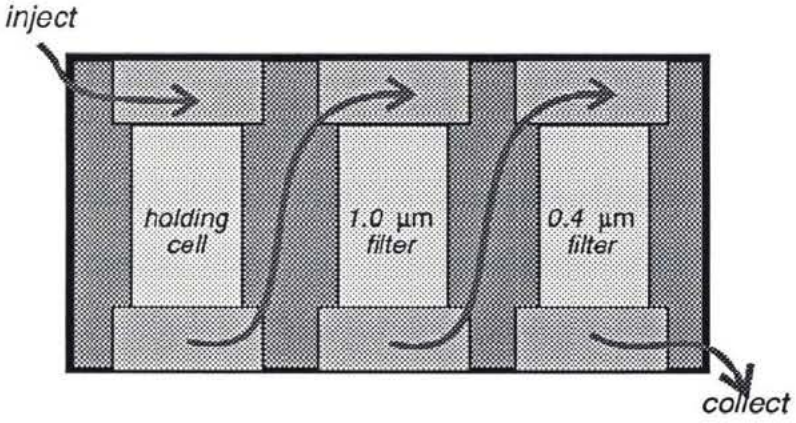

Figure 8 Vesicle Sizing/Filtration Unit

into the first cell. Use 10 psig nitrogen gas to force the vesicle solution through the first filter. Higher pressure may be required to force the solution through the second filter. The slower the filtration, the better the sizing of the vesicles; have the solution filter at 1 or 2 drops per second.

Equilibrate the Sephadex G-25M disposable columns with 10 mL of the external solution. Load all of the vesicle solution. There will be three fractions: 1) multi-lamellar vesicles (MLVs); 2) large unilamellar vesicles (LUVs) (the desired fraction); and 3) small lipid aggregates and excess internal solution. There is a dead volume of 2.5 mL, and the first 15 drops of the vesicle band must also be discarded (contains mostly MLVs.) Watch for a cloudy "doughnut" to form in the clear eluent in the receiving vial - this is the front of the vesicle band. Collect the next 4.5 mL of vesicles.

The prepared vesicles can be made and used on the same day, or used for the next two days. Batch-to-batch reproducibility is a problem, and within one batch there are differences noted for use over the 72 hour usable lifetime of the vesicles. It appears best to use the entire batch within 36 hours of its preparation.

Phospholipid Concentration Analysis

Complexation of the phosphate headgroups of the phospholipid with a visible light absorbing species, phospho-molybdate, allows quantitative analysis of its concentration.

Solutions

Solution 1 - 16.00 g ammonium molybdate·$4H_2O$, 120.0 mL D^3 H_2O.

Solution 2 - 80.0 mL Solution 1, 40.0 mL concentrated hydrochloric acid, 10.0 mL mercury. After stirring for 30 minutes, three layers will separate upon standing for 5 minutes.

Solution 3 - all the filtrate of solution 2, remaining portion of solution 1, 200.0 mL concentrated sulphuric acid.

Chromogenic acid solution - 25 mL solution 3, 45 mL methanol, 5 mL chloroform, 20 mL water. These solutions have approximately a six month shelf life if kept in glass bottles and

refrigerated.

Procedure

Transfer 50 µL of vesicle solution into a large 1.5 cm diameter test tube. The vesicle solution has a typical concentration of about 10 $mg{\cdot}mL^{-1}$ phospholipid (thus, approximately 0.5 mg phospholipid is being analyzed). Transfer appropriate quantities of the vesicle stock solution in chloroform into three test tubes to cover the range 0 - 1 mg phospholipid (at 50 $mg{\cdot}mL^{-1}$ use 0 - 20 µL). Add 0.4 mL chloroform and 0.1 mL of the chromogenic solution; boil for 1 minute for all test tubes. Cool to room temperature. Add 4 mL chloroform, shake gently, and wait 30 minutes. Carefully pipette out the chloroform layer into a 1 cm quartz cell, and record the UV absorption at 710 nm. The blank is 50 µL of chloroform as the solution aliquot in the procedure. The concentration of the vesicle solution can be extrapolated from a Beer-Lambert plot.

Microscopic Analyses

The following materials were purchased from the University of Victoria electron microscopy laboratory: Formvar, phosphotungstic acid, 150 mesh copper grids, microscope slides, and slide dipping tank.

Solutions

Formvar solution - 0.04 g Formvar, 10.0 mL chloroform; filter into dipping tank.

Staining solution - 2% (w/w) phosphotungstic acid (PTA) in water; adjust pH to 7.2 using 5 M potassium hydroxide; make in 50 mL batches.

Preparation of Grids

Dip a microscope slide half of its length into the Formvar solution in the dipping tank. Remove after 20 seconds and let dry for 30 minutes. With a razor blade, cut the dried Formvar film close to the leading edge, across the entire width of the slide, one side only. Lift the leading edge of the film off the slide by blowing moist air parallel to the plane of the slide. Fill a 20 cm diameter Petri dish with water. Dip the slide at a shallow angle, cut film side

up, into the water. The hydrophobicity of the film will force it to float on the surface of the water once it detaches from the slide. Make sure the film is floating and completely detached from the slide before continuing.

Using tweezers, place the copper grids dull side down on the floating Formvar film no closer than 2mm apart. Carefully place a fresh piece of Parafilm (large enough to easily cover the Formvar film) on top of the film/grids; the film will stick to the Parafilm. Remove and dry, grid side up, and protect from dust.

Loading and Staining

Place a drop of vesicle solution on the Formvar covered side of a prepared grid. After 20 seconds lift the grid with tweezers, and remove the excess solution by placing it to the edge of a filter paper.

To stain the vesicle grid, put a drop of phosphotungstic acid solution on a piece of Parafilm and place the grid, vesicle layer down, on the drop for 30 seconds. Remove the grid from the stain and remove the excess staining solution by placing the grid to the edge of a filter paper. Dry the grid under a hot lamp for 2-3 minutes.

Transmission Electron Microscope Analysis

Under the microscope the vesicles appear as round, dark objects on a pale background (see Figure 9). Their size distribution and number of lamellae can be determined by examination of photomicrographs taken using the microscope.

The pH-stat Experiment

Valinomycin, carbonylcyanide-trifluoromethoxyphenylhydrazone (FCCP), gramicidin D, amphotericin, Triton X-100, and the sulphate salts of potassium, sodium, lithium, rubidium, and cesium, were purchased from Sigma/Aldrich.

Valinomycin, FCCP, and gramicidin D were dissolved in methanol to concentrations of 5.2 x 10^{-5} M, 7.7 x 10^{-4} M, 3.3 x 10^{-5} M, respectively. Amphotericin was dissolved to 2.3 x 10^{-4} M, in dimethylsulphoxide (Aldrich). Triton X-100 was diluted by a factor of 20 with D^3 water.

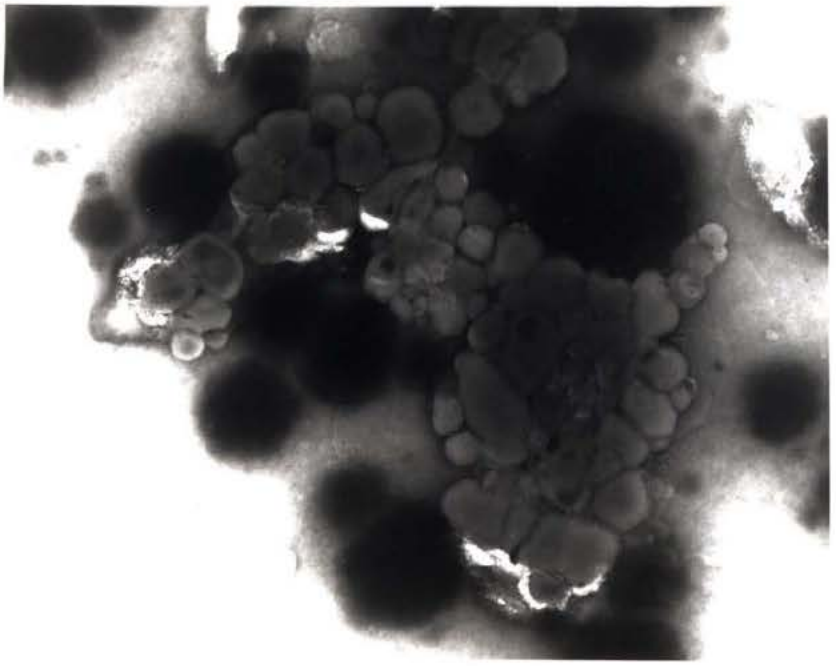

Figure 9 Transmission Electron Photomicrograph of Prepared Vesicles - magnification of 36,000x.

The $(G8TrgP)_6$ mimic was dissolved in methanol at a concentration of 4.0×10^{-4} M.

The following is a brief summary of the protocol used in this study. The vesicles were prepared with an entrapped buffer at pH 6.6. The buffer was composed of Bis-Tris, which was observed not to permeate nor be transported through the membrane. A one pH unit gradient was imposed by addition of the choline hydroxide titrant solution. A cation concentration gradient was created by adding a cation sulphate salt solution to the system. The transporter was then added, and the pH and cation gradients began to collapse. If necessary, a proton gradient decoupler (FCCP) is added if the transporter cannot achieve antiport translocation of the protons and cations. As the gradients collapse, the protons are released into the bulk solution and the pH drops. The titration instrumentation continuously adds sufficient choline hydroxide titrant to increase the pH to its initial point. The volume of base added versus time data was accumulated until the transport event was complete. The remaining protons were then released into the solution through lysis of the vesicles with Triton X-100, and were subsequently titrated. The data provided a rate constant for the release of protons from the vesicles which correlated with the translocation of the cations across the membrane.

The pH-stat Data Accumulation and Manipulation Program

The pH-stat program written for this project is divided into two parts. The first part of the program deals with the accumulation of time versus volume data, allows for changing the time delay, and records time events as required by the operator. The second part of the program is for data manipulation: re-calling, re-plotting, linear and first order regression.

The first order rate equation for the time versus volume curve generated by the pH-stat experiment is determined with minimal operator intervention. The operator defines the initial and final times of the experiment, then chooses a secondary initial time to create a new time range for the data manipulation (this is to overcome the lag-time experienced by the titrimeter when dealing with a fast titration). The operator then enters a low/high delta volume value for the titration, and enters a positive/negative increment volume value to guide the program's search for the best fit to the data. The algorithm is based on comparing the regression coefficients generated by changing the delta volume of the titration; there will be a maximum value of the regression coefficient corresponding to the best fit equation for the data. The algorithm is:

enter record number of time and volume initial $\rightarrow V_0$

enter record number of secondary time initial

enter record number of time final

enter estimate of delta volume for titration (ΔV)

enter increment volume value

LOOP 1: determines record number of maximum volume allowable for the titration since logarithm of negative numbers not allowed

LOOP 2: determines coefficients (slope, y-intercept, and regression) of the graph:

time elapsed versus $\ln(1 - (V_{t.e.} - V_0)/(\Delta V))$

for the time range specified by the secondary time initial and the time at which the maximum volume allowable was reached

IF present r^2 value lower than previous r^2 value

THEN best fit has been found (i.e. previous value of delta volume)

ELSE apply increment to delta volume and GOTO LOOP 1

A graph of the manipulated data and first order line is printed out, along with the constants and variables involved.

RESULTS AND DISCUSSION

Part I General Results

Egg L-α-lecithin vesicles were prepared by reverse evaporation. The crucial step in the preparation was the sonication. The goal was to produce monodispersed large unilamellar vesicles with high entrapment efficiencies and low permeation rates for high quality pH-stat experiments. Variation of the sonication period affected the size of the vesicles. Long sonication times broke down the dispersion into smaller water-in-oil droplets; short periods did not disperse the droplets sufficiently. The sonication was on a pulse by pulse basis until the solution became a translucent gray. The evaporation of the ether from the mixture needed attention and short duration. Complete removal of the ether was essential, but loss of water had to be minimalized. Extra internal buffer solution was added to the gel if it appeared to be drying instead of collapsing to the liquid; short periods of vortex mixing also assisted the collapse. The filtration and size chromatography procedures did not require special attention. Day-to-day and batch-to-batch variability was an ongoing problem. Vesicles were continually assessed both qualitatively and quantitatively.

The quality of the vesicles was judged several ways: electron microscopy, to measure size distribution; phospholipid concentration analysis, to calculate lipid and vesicle concentration; and, melittin versus Triton X-100 lysis, to determine the percentage of entrapped buffer in uni- versus multi-lamellar vesicles. The average size of the vesicles was 1200 Å, as determined from the transmission electron micrographs. About 5% of the vesicles were between 2500 and 3500 Å, and 5% were less than 600 Å. There was also a large amount of what appeared to be a small lipid aggregate (see Figure 9). The melittin assay[15] determines the portion of entrapped buffer that is within unilamellar vesicles. Melittin can enter and rupture only one level of bilayer per dose into the solution. The assay requires addition of a single dose of melittin concentrated enough to affect all vesicles in the solution followed by detergent lysis of all remaining vesicles. The vesicle solutions were assessed as having 95 % of the entrapped

buffer within unilamellar vesicles. Thus, the aggregate lipid had very little, if any, entrapped buffer. The phospholipid concentration was typically 1.9 mg phospholipid per experiment. The calculated vesicle concentration (using average headgroup area as 50 $Å^2$ [37]) was 15 x 10^{12} per experiment. Taking into account the large quantity of aggregate or multilamellar vesicle present, it is possible that as little as a third of the calculated number of vesicles were capable of reporting transport events. Multilamellar vesicles are just as subject to transporter insertion as any other vesicle; the problem lies in their lack of entrapped buffer to report any transport that may occur.

The quantity of vesicle solution (0.2 - 0.3 mL) used in the pH-stat experiment varied between batches of vesicles because of the differences in vesicle size distributions and entrapment efficiencies. In order to acquire sufficient data per pH-stat experiment, the total entrapped volume of internal solution had to be large enough to titrate with the choline hydroxide titrant. Also, the entrapped protons were rarely completely released during a transport event. In practice, sufficient vesicles were used to produce a Triton lyse volume of 0.3 - 0.5 mL to regain the set pH. The goal of this procedure was to ensure sufficient entrapped internal buffer solution to result in a large enough data set for the transport event; greater than 100 data points for each experiment was a reasonable and routinely achieved goal.

Having established the quality of the vesicles in a batch, and the quantity required, external solution was added to the aliquot of vesicle solution to make a total of 4.0 mL in the cell. At this point, the pH in the cell was between 6.5 and 6.9 - due to the mixing of the external solution and the excess internal solution of the vesicle solution, carried through from the vesicle preparation. Since the internal solution pH was 6.60, the automatic titrimeter pH end-point was set to 7.60. Apparently, the pH gradient and subsequent rate were unrelated for set end-points between 7.55 and 7.80 pH. The titrimeter was then activated, and choline hydroxide titrant was added to create the one pH unit gradient across the vesicle membrane.

That titrant volume was recorded, as it provided a precise measure of the volume of the vesicle aliquot. The data acquisition of volume of titrant added versus time, began here.

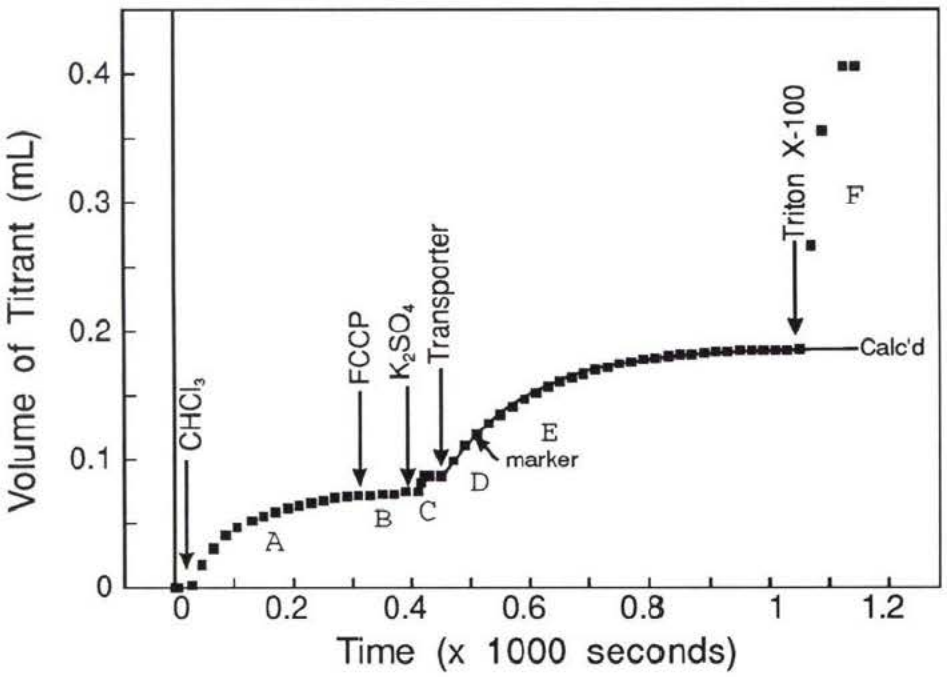

Figure 10 Typical Plot of Titrant Volume Added versus Time Elapsed for a pH-Stat Experiment - refer to text for detail.

The first additive to the cell was chloroform. On average, 15 µL was added to get a titration effect of about 0.070 mL, but some batches of vesicles required a larger or smaller aliquot of chloroform to provoke the same effect (see Figure 10, region A). The presence of chloroform was needed to induce the $(G8TrgP)_6$ mimic to function significantly above the lower limit of detection of the pH-stat experiment. The chloroform was an experimental convenience, and its effect was investigated. The more chloroform that is added, the greater its effect on the vesicles. More entrapped buffer is released, possibly due to lysis of some vesicles. Second, the greater the initial effect, the faster the rate of proton release from the vesicles during a $(G8TrgP)_8$ mimic transport experiment. At the concentration used, bulk chloroform is visibly present on the cell walls. Any lipid which is dissolved into the chloroform droplets is not party to the transport events. The faster the chloroform is added into the solution through a fine

syringe needle (i.e. the finer the dispersion), the greater the initial effect on the vesicles. These observations suggest that the addition of chloroform generated a population of vesicles, which either was more easily entered by the mimic, or allowed more rapid gating of the mimic. Other solvents were tested: hexane, ether, dichloromethane. Of these, hexane showed no effect, ether was required in large (0.25 mL) doses, and the dichloromethane acted similarly to the chloroform. Chloral hydrate, a water soluble general anaesthetic, was also added to the vesicles, but no effect was observed. Halothane, a volatile general anaesthetic, was tested; it acted similarly to chloroform in its ability to enhance the function of the $(G8TrgP)_6$ mimic. The effect of chloroform on the experimental results is discussed later in the text.

After the chloroform effect reached its plateau, the proton carrier $FCCP^2$, was added to the cell. Since neither the mimic nor valinomycin were apparently capable of cation/proton antiport, $FCCP^2$ was added to the membrane to maintain the electroneutrality of the transport event. Transport experiments using the $(G8TrgP)_6$ mimic used 1 µL aliquots of 0.766 mM FCCP; this gives in-cell molarities between 0.15 and 0.18 µM, depending on the volume of additives to the initial 4 mL cell volume. This amount of FCCP induced a small base rate when metal cations were present in the bulk solution and a transporter was not (less than 5×10^{-10} mol $H^+ \cdot s^{-1}$, or 0.025×10^{-2} s^{-1}). Proton transport by FCCP was not a rate determining factor since larger amounts raised only the rates observed for FCCP and cations alone, and not the rates observed for transport due to the $(G8TrgP)_6$ mimic. Valinomycin transport experiments used similar FCCP in-cell concentrations. Gramicidin did not require the use of FCCP; experiments with and without FCCP showed no difference in its transport rates. In the experiment of Figure 10, region B, there was no proton release due to the addition of the FCCP; this was a typical result.

For transport experiments of the $(G8TrgP)_6$ mimic, the metal cation was the next additive to the cell (see Figure 10, region C). The commercial sulphate salts of lithium, sodium, potassium, cesium, and rubidium were used at concentrations of 0.500 M, and the solutions

varied in their pH's. With the addition of rubidium sulphate to the cell, a large amount of titrant was required to regain pH 7.60. This was not due to antiport of rubidium and protons across the membrane, nor due to lysis of the vesicles, since the titrant volume for Triton lysis in that experiment was proportionally greater than for other lyses of that vesicle batch. If the addition of the metal caused the pH to drop below 7.60, then the titrant volume to regain the set pH was recorded and subtracted from the total lyse volume of that experiment. If the addition of the metal raised the pH above 7.60, then the titrimeter end-point was reset to that pH. An adjustment of less than 0.2 pH units was not great enough to increase the rate of titrant addition. The automatic titrimeter was stopped for the addition of cation until a steady pH was reached, so that unnecessary titrant was not added. These protocols were followed to establish a reproducible equilibrium in the cell before the transport event began.

Some of the valinomycin and gramicidin transport experiments had the sequence of addition of the metal cation and the transporter reversed. In these cases, the metal was potassium and the quantities added always induced a rise in the cell pH. Before addition of the potassium the titrimeter would be halted, as explained above, and immediately reactivated once the rise in cell pH was complete and the set pH adjusted. This method was more demanding of the experimenters' judgement; the first several seconds of the transport event may have been missed, but in general, the results did not vary from that calculated with the method described above.

The transporter was added next (see Figure 10, region D). The concentrations of the $(G8TrgP)_6$ mimic, valinomycin, and gramicidin are detailed in the data tables. The $(G8TrgP)_6$ mimic and valinomycin concentrations were similar, between 40 and 800 nM; gramicidin was needed between 0.3 and 13 nM only. The majority of the transport experiments required slow rates of addition of titrant to maintain the set pH; this addition was controlled by the buret and was always at the lowest speed setting. However, if the initial rate of proton release was very fast then the cell pH would drop and the titrimeter would be unable to catch up until the

rate slowed sufficiently. In that instance, the buret addition rate was manually increased until the titrimeter could maintain the pH-stat condition. When the titrimeter gained control of the cell pH, as evidenced by the cell pH remaining static at the set end-point, the data set was "marked" (beginning of region E) so that the initial rate data could be dealt with correctly. The total volume of titrant consumed by the transport event was unaffected (see Figure 10, regions D and E), but the data set used to determine the first order regression was truncated (region E) to include only that data acquired under titrimeter control of the cell pH.

After the transport event was complete (the addition rate of titrant leveled to zero), the remaining protons were titrated by lysing the vesicles with Triton X-100 (see Figure 10, region F). The volume of choline hydroxide used to titrate *all* available protons in the vesicles (lyse volume) was proportional to the entrapped volume of the vesicles' internal buffer, and provided a normalisation factor for between experiments.

The rate constant for the transport event was calculated according to a first order analysis. The algorithm for the determination of the observed rate constant, k_{obs}, is outlined in the experimental chapter. The absolute rate of moles of protons released per second was calculated by multiplying the rate constant by the volume of titrant used for the transport event and by the concentration of the titrant. The rates quoted throughout this report are normalized with respect to the lyse volume for each run. The volume of titrant used for the transport event is divided by the volume of titrant corresponding to the total available protons in the initial vesicle aliquot (lyse volume). This percentage of transported protons is multiplied by the rate constant to give a rate of protons released per second as a percent of the maximum protons available for transport, in units of 10^{-2} s^{-1}. The absolute values of the rates between batches of vesicles, and hence between most of the series of experiments, are not directly comparable (an estimated reproducibility of ± 20%), but the general trends observed and the large differences between rates are comparable.

The lower limit of detection of transport was 0.02×10^{-2} s^{-1}, this was usually attributed to

a leakage rate due to vesicle aging. The dynamic range of the experiment was (0.02 - 4.0) x 10^{-2} s^{-1}, but the most reliable and reproducible rates (± 10%) were in the range 0.06 - 0.8 x$10^{-2}$$s^{-1}$. The precision of duplicate runs was usually better than ±10%. Exceptions to this were not common, never greater than ±30%, and are noted in the data tables. The concentration of the choline hydroxide titrant was 4.75 ± 0.01 mM for the majority of the experiments, except for experiments of data Table V, Table XI, Table X and Table XV, where the titrant concentration was 3.98 ± 0.02 mM. Chloroform was not used in all the experiments, and its absence is noted in the data tables.

Part II Experimental Results

The data set for each transport event was analysed to determine the apparent first order rate constant, as outlined in the experimental section. The constant multiplied by the titrant volume required to complete a transport event, and by the concentration of the choline hydroxide titrant, gave a rate of moles of protons released per second into the cell solution. What do these rates actually mean? Their literal interpretation is the rate of addition of choline hydroxide into the cell to titrate the protons released from the vesicles. This is a result of monovalent metal cations crossing into the vesicles. Following Gary-Bobo[2], the observed rate also reflects the translocation of cations across the membrane. The control experiments showed that in the absence of transporter the protons were released at a very slow rate when both FCCP, the proton carrier, and the cation were present. This rate remained low even at high cation concentrations. The rate only increased if the transporter was present. In the cases of the mimic and valinomycin, transport *did not occur* without FCCP; therefore, these transporters do not mediate proton transport with any detectable efficiency. In contrast, gramicidin was able to facilitate antiport of protons and cations. The net conclusion is that the observed rates reflect the proton and metal cation antiport across vesicle bilayers.

How do the observed rates determine the mechanism of the mimic? Individually, no rate serves to establish the mimic's mode of action, but collectively they evaluate properties of the mimic which serve primarily to establish the mimic as a transporter, and then to relate its mode of action to either gramicidin - a channel[1], or valinomycin - a carrier[2].

The procedure outlined in Part I was followed as closely as possible to create reproducible conditions for all the experiments designed to characterize the $(G8TrgP)_6$ mimic. All the experiments could not be done using a single batch of prepared vesicles, since 24 runs per preparation was the maximum ever realized. Therefore, each property of the $(G8TrgP)_6$ mimic was determined from a set of experiments run within one batch of vesicles. Some batches of vesicles allowed two aspects of the mimic to be examined and compared, but between batch

comparisons were rarely used. The $(G8TrgP)_6$ mimic was characterized according to its: 1) concentration dependence; 2) temperature dependence; 3) cation selectivity; 4) dependence on potassium and cesium concentration; 5) response to octylammonium concentration as an inhibitor of potassium transport; and 6) activity in membrane conductivity experiments.

Concentration Dependence

The concentration dependence of transport by the $(G8TrgP)_6$ mimic was studied and compared to gramicidin D and valinomycin (see Table I, Table II, and Table III). Figures 11, 12, and 13 are the experimental data curves for the pH-stat titrations induced by the mimic, gramicidin, and valinomycin. The experiments were designed to determine the kinetic order of the transporter by the method of initial rates. The concentration of the transporter was varied over at least two orders of magnitude while all other concentrations remained constant. The cation concentration was within its saturation range so that variation in the solution volume would not affect transport rate due to variation in cation concentration.

Table I

Dependence of k_{obs}, Extent of Transport, and Overall Rate as a Function of the Concentration of $(G8TrgP)_6$ Mimic

$(G8TrgP)_6$ mimic Concentration	[a]k_{obs}	Extent of Transport	[b]Rate
$x10^{-7}$ M	$x\ 10^{-3}\ s^{-1}$	%	$x\ 10^{-2}\ s^{-1}$
0.0	9.8^3	3	0.03
0.4	7.2^0	7	0.05
0.8	5.6^7	18	0.10
2.0	5.7^0	22	0.12
4.0	5.1^5	30	0.16
4.0	4.5^7	37	0.17
8.0	5.7^3	29	0.17
8.0	4.7^0	36	0.17
8.0	6.9^5	26	0.18

a) 25°C; $[K^+]$ = 95 mM; [FCCP] = 0.16 μM; r^2 values for fit to first order regression >0.999.
b) rate expressed as percent H^+ available transported per second; absolute rate for $2\ x10^{-7}$ M (transport volume = 0.104 mL of 4.75 mM choline base) was $28\ x\ 10^{-10}$ mol $H^+ s^{-1}$.

The data curves were normalized to compensate for the heterogeneity of the vesicle solution. Since the number of vesicles varied between the aliquots of the vesicle solution

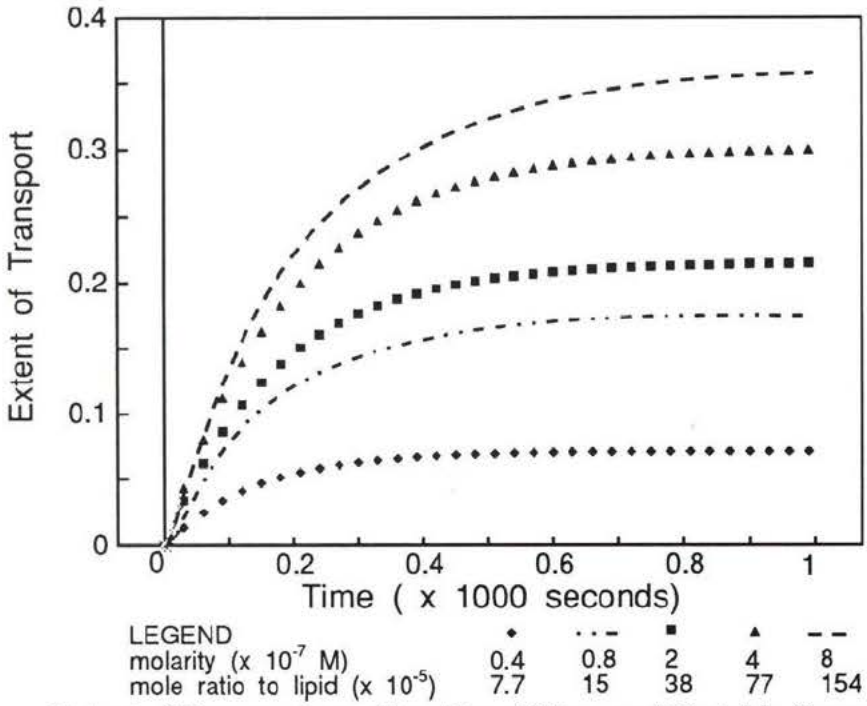

Figure 11 Extent of Transport as a Function of Time and Variable Concentrations of $(G8rgP)_6$ Mimic

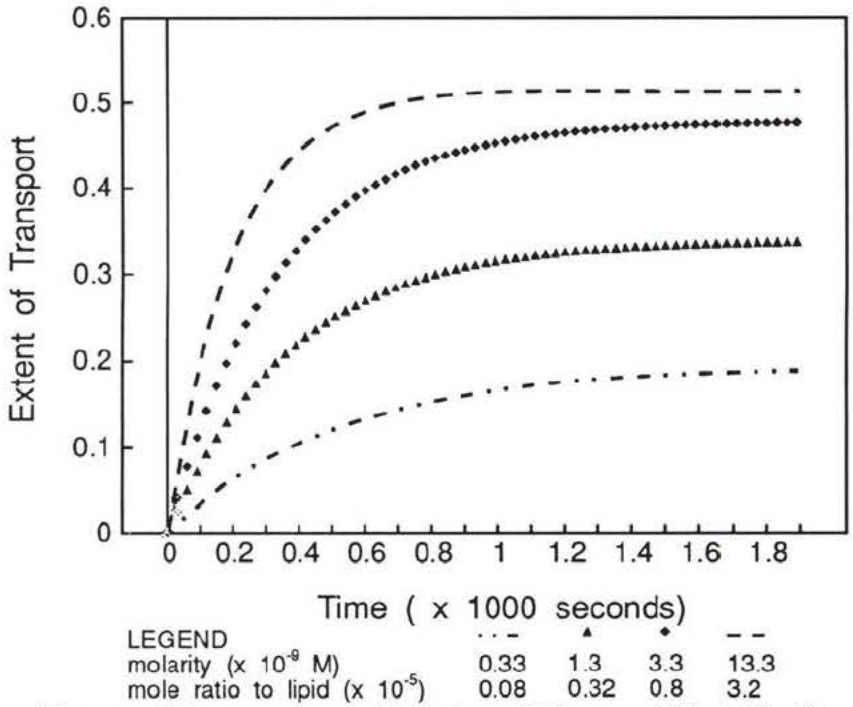

Figure 12 Extent of Transport as a Function of Time and Variable Concentration of Gramicidin

added to the cell, and the transport event depended upon the distribution of transporter into the vesicles, then the titrant volumes associated with the transport event and the total vesicle

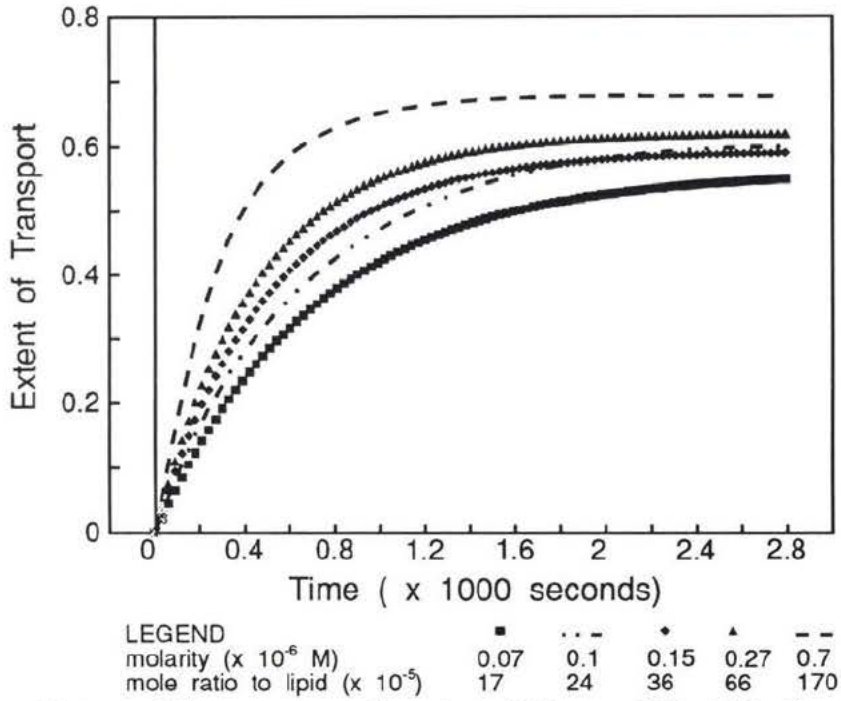

Figure 13 Extent of Transport as a Function of Time and Variable Concentrations of Valinomycin

lysis varied. As described above, dividing the titrant volume used for the transport event (transport volume) by the titrant volume for total vesicle lysis (lyse volume) normalized the curves to reflect the rate of release of protons from the vesicles as a percent of the total available protons within the vesicles.

The data curves displayed were generated using the slopes and volumes calculated from a first order linear regression applied to the accumulated time versus volume data. They were used in place of the actual data curves to simplify the normalization calculations and graphic presentation. For the mimic and valinomycin, the generated curves closely matched the experimental data (see Figure 10), the calculated line is visually indistinguishable from the experimental data of regions D and E). The correlation coefficients (r^2 values) from the linear regression exceeded 0.99 in these cases. For gramicidin, the generated curves matched the actual data less closely, but linear regression resulted in r^2 values exceeding 0.97.

The concentrations of transporter used are specified in each figure. They are not of the same magnitude since the mimic is much less active than gramicidin. A very low

Table II

Dependence of k_{obs}, Extent of Transport, and Overall Rate as a Function of the Concentration of Gramicidin

Gramicidin Concentration	[a]k_{obs}	Extent of Transport	[b]Rate
$x10^{-9}$ M	$x10^{-3}$ s^{-1}	%	x 10^{-2} s^{-1}
0.3	1.4^{0}	19	0.03
1.3	2.2^{0}	34	0.08
3.3	3.2^{5}	48	0.16
6.6	4.6^{0}	51	0.24
13.3	4.6^{0}	50	0.23

a) 25 °C; $[K^+]$ = 43 mM; [FCCP] = 0; r^2 values for fit to first order regression were >0.98; no chloroform used.
b) rate expressed as percent H^+ available transported per second; absolute rate for 13.3 x 10^{-9} M gramicidin (transport volume was 0.130 mL of 4.75 mM choline base) was 33 x 10^{-10} mol $H^+ \cdot s^{-1}$.

concentration of the mimic gave a rate below the detection range of the experiment. Conversely, a high concentration of gramicidin induced rapid transport too fast for the pH-stat experiment to follow accurately. The concentrations used produced rates between 0.04 and 0.80 x 10^{-2} s^{-1}, within the dynamic range of the experiment. The lowest transport rates used were 2 - 3 times above the leakage rate; thus, corrections were not applied.

Each of the figures show a general increase in rate for an increase in transporter concentration. This is consistent with distribution of the transporter into progressively larger populations of vesicles[2]. The figures showing mimic and gramicidin concentration dependence also show a trend of increasing transport volume for increasing concentration. This trend was observed previously by Gary-Bobo[2]. This is not observed in the valinomycin graph; here the delta transport volume is constant, within experimental error (± 10%) (also observed previously[2]). This suggests that valinomycin is able to move between vesicles. The increase in rate for an increase in valinomycin concentration simply indicates the broader initial distribution of the transporter into the vesicles before it moves between vesicles. Gramicidin

Table III

Dependence of k_{obs}, Extent of Transport, and Overall Rate as a Function of the Concentration of Valinomycin

Valinomycin Concentration	[a]k_{obs}	Extent of Transport	[b]Rate
x 10^{-8} M	x10^{-3} s^{-1}	%	x 10^{-2} s^{-1}
0	1.2^{3}	59	0.07
7	1.4^{0}	56	0.08
10	1.5^{0}	61	0.09
15	1.9^{5}	59	0.12
27	2.2^{0}	62	0.14
64	2.8^{3}	73	0.20
68	3.1^{3}	76	0.24
68	3.4^{0}	67	0.23
68	3.3^{0}	69	0.23
170	5.2^{5}	78	0.41

a) 20 °C; $[K^+]$ = 53 mM; [FCCP] = 0.16 μM; r^2 values for fit to first order regression were >0.999 (except for [valinomycin]=0, r^2=0.98); no chloroform used.
b) rate expressed as percent H^+ available transported per second; absolute rate for [valinomycin] = 68 x 10^{-8} M (transport volume was 0.198 mL of 4.75 mM choline base) was 31 x 10^{-10} mol $H^+ \cdot s^{-1}$.

and the mimic apparently enter a population of vesicles and remain there.

To establish that these two transporters do not move between vesicles "add back" experiments were run. The "add back" experiment followed this sequence of steps: The vesicle solution and external solution were added to the cell and brought to the set pH as in a normal experiment. Chloroform, FCCP, and potassium sulphate were added to the cell and the solution allowed to equilibrate. Before the transporter was added, 1.4 mL of the solution was removed and kept in a glass syringe. The transporter was then added to the cell and the transport event was allowed to go to completion. At this point, the 1.4 mL sample was added back into the cell. There was an instantaneous drop in pH due to the base rate which had been occurring, unchecked, in the syringe solution. The pH in the cell was brought to the set

pH and observation of any additional transport events began. In both cases, gramicidin and the mimic showed less than 10% of the expected rate. There was not sufficient transport rate nor extent of transport to indicate that transporter remained in the bulk solution, thus eliminating the possibility of poor partitioning to the vesicles from the bulk solution.

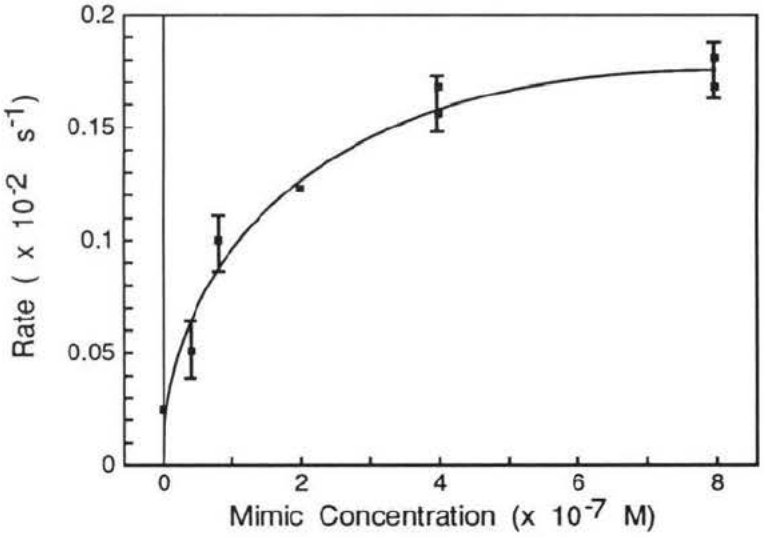

Figure 14 Dependence of Rate on Concentration of $(G8TrgP)_6$ Mimic

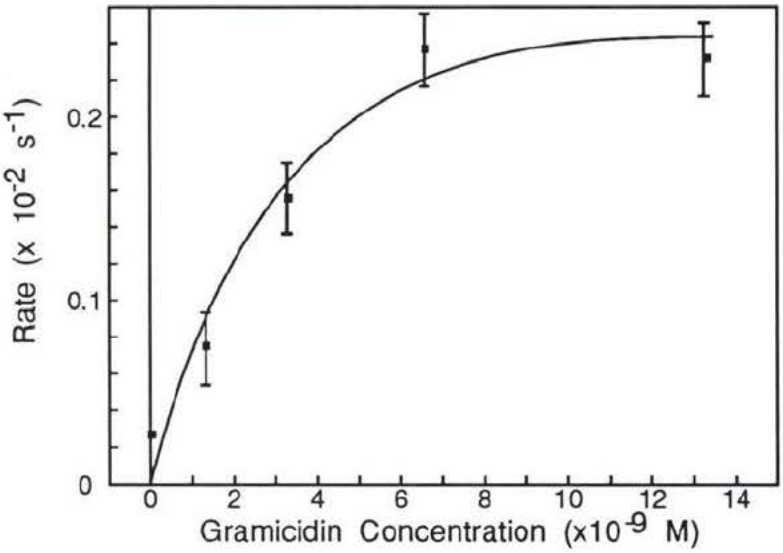

Figure 15 Dependence of Rate on Concentration of Gramicidin

Both the mimic and gramicidin reached a saturation rate at high concentrations, as

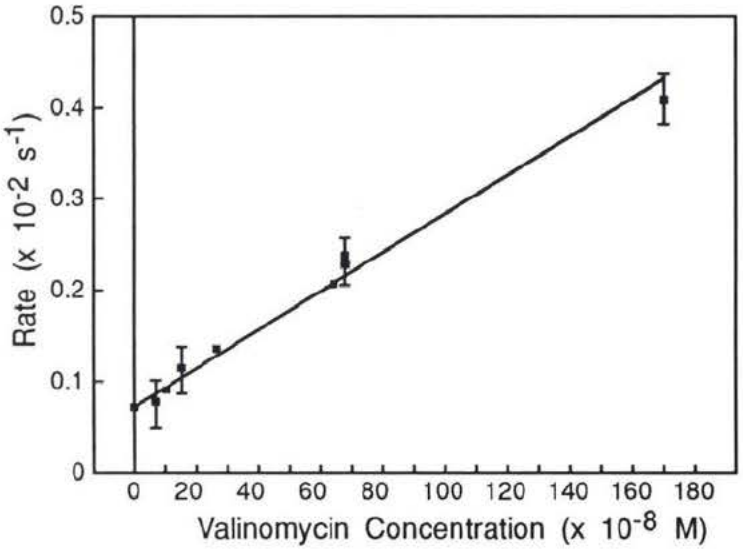

Figure 16 Dependence of Rate on Concentration of Valinomycin
- linear regression of rate versus concentration data gave $r^2 = 0.986$.

presented in Figures 14 and 15. The curves have been drawn in to aid visual interpretation of the data. The graphs of rate versus concentration of transporter show at "low" concentrations there was a rough linear relationship, but that a plateau was achieved at higher concentrations. This is consistent with greater numbers of vesicles becoming populated by transporter molecules, up to a limit. This is different from the effect of higher concentrations of valinomycin, as displayed in Figure 16; here the increase in concentration increases the rate of transport with no apparent saturation.

Based on the analyses of the vesicles used to obtain the gramicidin concentration dependence (1.5 mg phospholipid per experiment, 1250 Å average size, 50 $Å^2$ per headgroup), the concentration of vesicles was approximately 3×10^{-9} M. Thus, the data for gramicidin indicated that saturation occurred between 2 and 4 molecules per vesicle (not chloroform "softened"), assuming an even distribution. It is known that two molecules of gramicidin are required to form a channel[1] through a bilayer membrane. Since the saturation occurred at the concentration required to form one channel per vesicle then the linear portion of the concentration curve was due to the increased number of vesicles having whole channels. The

addition of more than 2 gramicidin molecules per vesicle did not increase the proton release rate, despite the obvious assumption that more channels were formed. This infers that one channel is sufficient to equilibrate one vesicle[2], and that its "open" lifetime is long enough to allow the transport of about 5 x 10^4 ions[a] across the membrane. The transport is therefore much faster than the gating rate of the gramicidin channel[2].

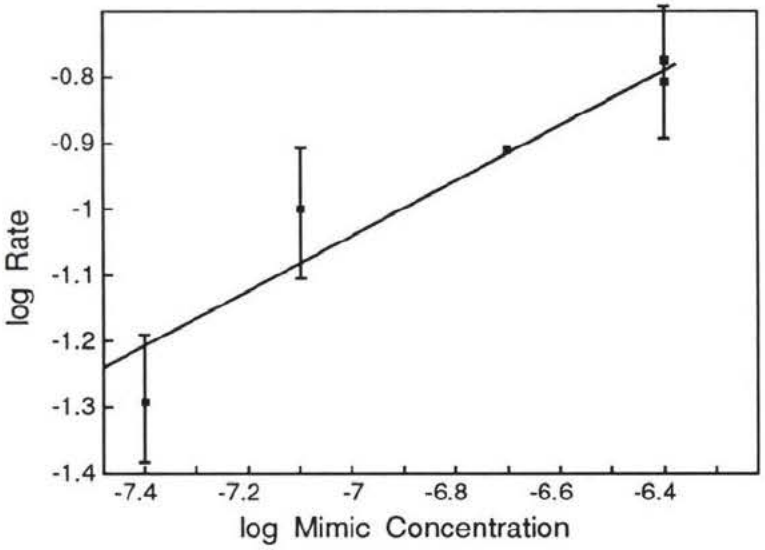

Figure **17** $(G8TrgP)_6$ Mimic: log Rate versus log Concentration

As was mentioned in the introduction, the mimic being studied in this report is an analogue to the molecule first prepared by Dutton[25]. The studies performed on that first molecule were along the lines of the current study; that is, its behaviour was compared to gramicidin and valinomycin. However, that study could not be completed, due to sample degradation. The current mimic was prepared by James, and the study was continued. It became apparent that the vesicle preparations were not the same as those previously used. For example, the James mimic required chloroform to give rates within the dynamic range of the experiment, and gramicidin required more than ten times its previous concentration to

[a] the volume inside a 1250 Å vesicle, 40 Å thick, is 8.4 x 10^{-19} L; the internal buffer concentration is 0.20 M, about half this concentration reflects the number of protons released to bring the internal pH of 6.6 to 7.6.

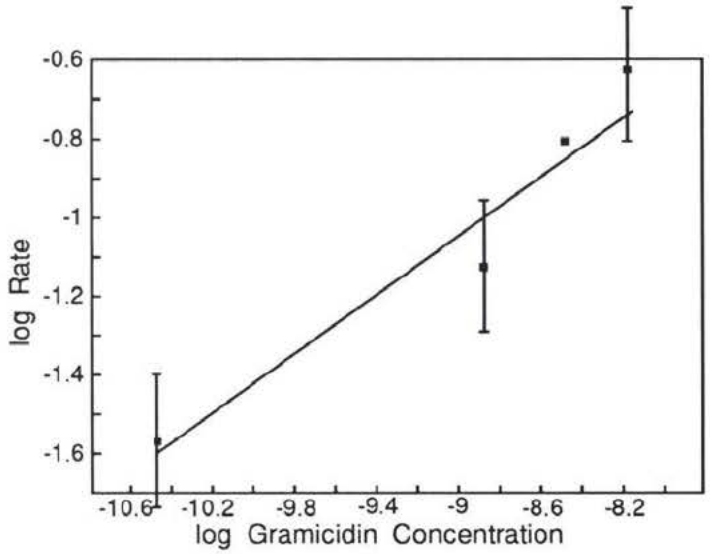

Figure **18** Gramicidin: log Rate versus log Concentration

achieve a saturation rate. The difference between the vesicle preparations was not an increase in the number of vesicles, but appeared to be a decrease in the fluidity of the membrane. The cause of the difference in the vesicles could not be determined, nor could the previous vesicle type be attained a second time. Most of the examination of gramicidin and valinomycin had been completed in the first study. A short survey into the behaviour of gramicidin and valinomycin indicated that the *mechanistic trends* previously observed had not changed, only the absolute rates had decreased. Since the mechanism of the mimic was to be inferred by comparison to the *behaviour* of gramicidin and valinomycin, some of that data was not duplicated in the current vesicle system. The distinction between the two sets of data is indicated by the presence or absence of chloroform "softened" vesicles in the experiment; chloroform only having been used in the most recent study.

The apparent kinetic order of the transporters was determined by the method of initial rates, following the equations below. The logarithm (base 10) of the rates was plotted against *the logarithm of the concentrations (see Figures 17 and 18). The log-log graph was not* produced for valinomycin since the rate was linearly proportional to concentration, as shown in Figure 16. Method of Initial Rates:

$$\text{rate} = k_{obs} * [A]^a * [B]^b * [C]^c * \ldots * [N]^n$$

$$\log \text{rate} = \log k_{obs} + a*\log[A] + \ldots + n*\log[N]$$

For the graph of log rate versus log[A], the slope, and the apparent kinetic order of A, is **a**, when all other concentrations and variables are constant. The orders of the mimic, gramicidin, and valinomycin are 0.45 ± 0.07 (r^2 = 0.92), 0.39 ± 0.07 (r^2 = .96), and 0.50 ± 0.07 (r^2 = 0.98), respectively. These results are ambiguous with respect to determining mechanistic differences.

Temperature Dependence

Study of the temperature dependence of the $(G8TrgP)_6$ mimic, gramicidin, and valinomycin provided a comparison of their Arrhenius activation energies (see Table IV, Table V and Table VI). Figure 19 shows the pH-stat experimental data for the mimic at temperatures ranging from 5 to 35°C. The concentrations of the mimic and potassium ion were within their saturation ranges: 8×10^{-7} M and 40 mM. The chloroform effect changed with the temperature: the higher the temperature, the greater the initial effect on the vesicles. Since the transport rates varied with the chloroform effect, the amount of chloroform added to the cell was modified to produce a similar chloroform effect for each temperature. However, this task proved very difficult, and only for this set of data was a normalizing factor of the chloroform effect applied to the rate determination. The rates were normalized to 0.056 mL for the initial chloroform effect. This normalization was used only in the calculation of the temperature dependent rates for the mimic. The difference in the activation energy for normalized versus "unnormalized" data was only 1.2 kJ/mol, but the error bars were slightly reduced by the normalization.

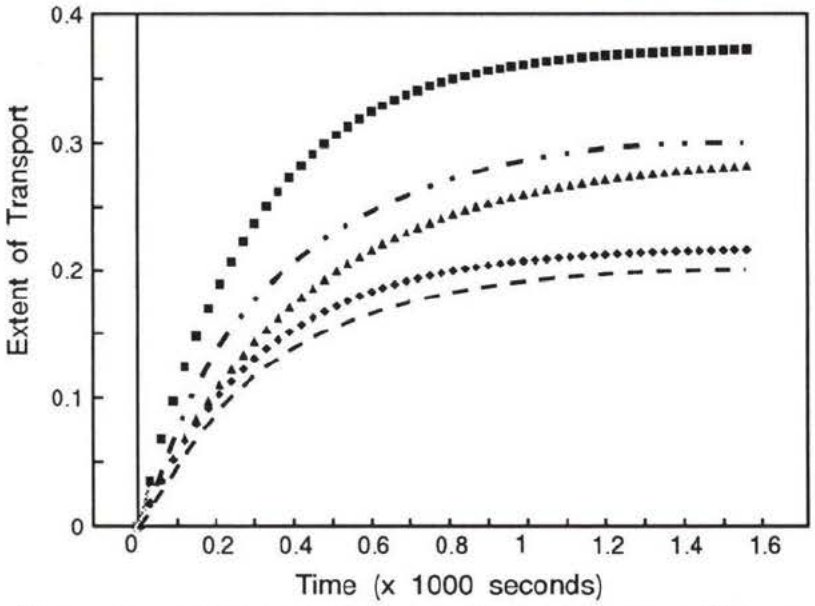

Figure **19** Dependence of Extent of Transport as a Function of Temperature for the $(G8TrgP)_6$ Mimic - for temperatures 5(--), 9(♦), 23(▲), 29(---), 35(■) °C.

Table IV

Dependence of k_{obs}, Extent of Transport as a Function of Temperature, and Overall Rate as a Function of the Volume Effect of Chloroform: $(G8TrgP)_6$ Mimic

Temperature	[a]k_{obs}	Extent of Transport	Volume Effect of Chloroform	[b]Rate
°C	x $10^{-3}s^{-1}$	%	µL	x 10^{-2} s^{-1}
5	2.8^{7}	20	87	0.04
9	2.2^{7}	29	62	0.06
17	3.7^{0}	40	121	0.07
23	3.0^{3}	22	49	0.08
23	3.0^{5}	17	48	0.06
23	3.7^{5}	44	132	0.07
29	2.8^{0}	30	56	0.09
35	3.3^{5}	38	67	0.11
35	2.5^{3}	36	69	0.07
35	2.5^{0}	34	58	0.08

a) [$(G8TrgP)_6$ mimic] = 8 x 10^{-7} M; [K^+] = 41 mM; [FCCP] = 0.16 µM; r^2 values for fit to first order regression were >0.999.
b) rate expressed as percent H^+ available transported per second; the chloroform volume effect was affected by temperature - as the effect increased so did the observed rate; therefore, the extent of transport was multiplied by 56 µL and divided by the volume effect observed for that run. This normalizes the rates with respect to the chloroform effect. The absolute rate for T = 29 °C (transport volume was 0.174 mL of 4.75 mM choline base) was 23 x 10^{-10} mol $H^+ \cdot s^{-1}$.

Figures 20, 21, and 22 are the Arrhenius plots for the mimic, gramicidin, and valinomycin. The temperature studies were conducted under different conditions. Gramicidin and valinomycin did not require chloroform "softened" vesicles to function, and their activation energies were determined to be approximately 24.5 ± 4.6 and 46.8 ± 6.6 kJ/mol without chloroform present. However, with chloroform present the activation energy of gramicidin decreased to 16.1 ± 1.7; the data for the determination of valinomycin in "softened" vesicles was unacceptable - there was no correlation (r^2 = 0.2) between temperature and rate. The activation energy for the mimic was 16.0 ± 3.4 kJ/mol in the presence of chloroform. Each of

Table V

Dependence of k_{obs}, Extent of Transport, and Overall Rate as a Function of Temperature: Gramicidin

Temperature	[a]k_{obs}	Extent of Transport	[b]Rate
°C	x 10^{-3} s^{-1}	%	x 10^{-2} s^{-1}
6	2.9^{7}	38	0.11
6	3.9^{3}	35	0.12
6	3.1^{0}	32	0.10
11	3.0^{3}	42	0.13
19	3.7^{0}	41	0.15
27	3.2^{3}	52	0.17
35	3.7^{0}	62	0.23
35	5.1^{3}	40	0.21

a) [gramicidin] = 6.6 x 10^{-9} M; [K^+] = 80 mM; [FCCP] = 0; r^2 values for fit to first order regression were ≈0.99.
b) rate expressed as percent H^+ available transported per second; absolute rate for T = 35 °C (transport volume was 0.132 mL of 3.98 mM choline base) was 17 x 10^{-10} mol $H^+ \cdot s^{-1}$.

the energies derived from the studies using chloroform are very low; the mimic and gramicidin energies are essentially identical and of the order of thermal energies in this temperature range.

The low activation energy for gramicidin is not surprising. One study of the effect of crystalline versus gel phases of the membrane on the effectiveness of channels and carriers[36] suggested that the activation energies of carriers and channels differ depending on the state of the bilayer. Above the phase transition, valinomycin transport rates were dependent on temperature, but below the bilayer melting point there was no temperature dependence and the rates themselves were negligible. For gramicidin, there was temperature dependence below the phase transition; above, there was no dependence, and the rates were essentially independent of temperature. Even with the chloroform present, the activation energies determined in this study appear to concur with these findings for transport through bilayers

Table VI

Dependence of k_{obs}, Extent of Transport, and Overall Rate as a Function of Temperature: Valinomycin

Temperature	[a]k_{obs}	Extent of Transport	[b]Rate
°C	x 10^{-3} s^{-1}	%	x 10^{-2} s^{-1}
10	1.2^{3}	19	0.02
15	1.7^{5}	22	0.04
20	1.6^{3}	33	0.05
20	1.5^{7}	38	0.06
20	1.6^{0}	41	0.07
25	1.5^{5}	52	0.08
30	1.7^{7}	48	0.09

a) [valinomycin] = 1.05 x 10^{-7} M; [K^+] = 44 mM; [FCCP] = 0.16 µM; r^2 values for fit to first order regression were >0.99; no chloroform used.
b) rate expressed as percent H^+ available transported per second; absolute rate for T = 30 °C (transport volume was 0.118 mL of 4.75 mM choline base) was 9.9 x 10^{-10} mol $H^+ \cdot s^{-1}$.

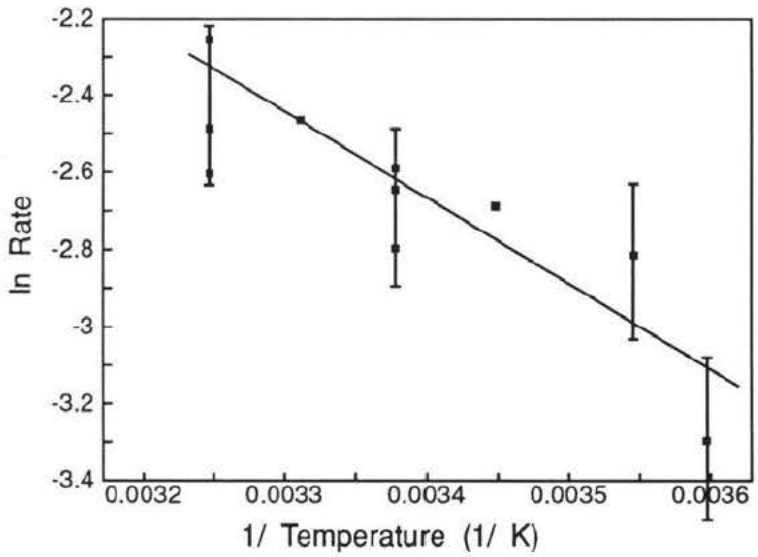

Figure 20 Arrhenius Plot: $(G8TrgP)_6$ Mimic
- activation energy E_{act} = 16.0 ± 3.4 kJ/mol, r^2 = 0.733.

in the gel phase; there is no phase transition for egg lecithin and cholesterol mixtures[44], thus the bilayer is always in a gel phase. Relating the $(G8TrgP)_6$ mimic to gramicidin and

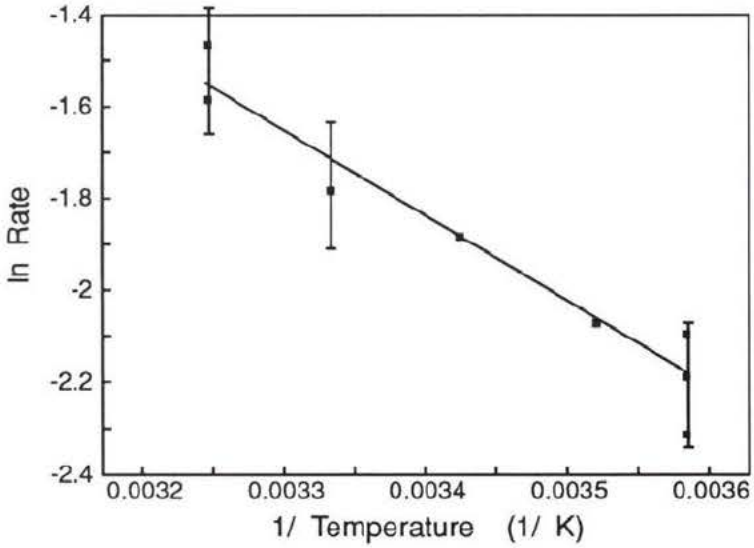

Figure 21 Arrhenius Plot: Gramicidin
- activation energy E_{act} = 16.1 ± 1.7 kJ/mol, r^2 = 0.941.

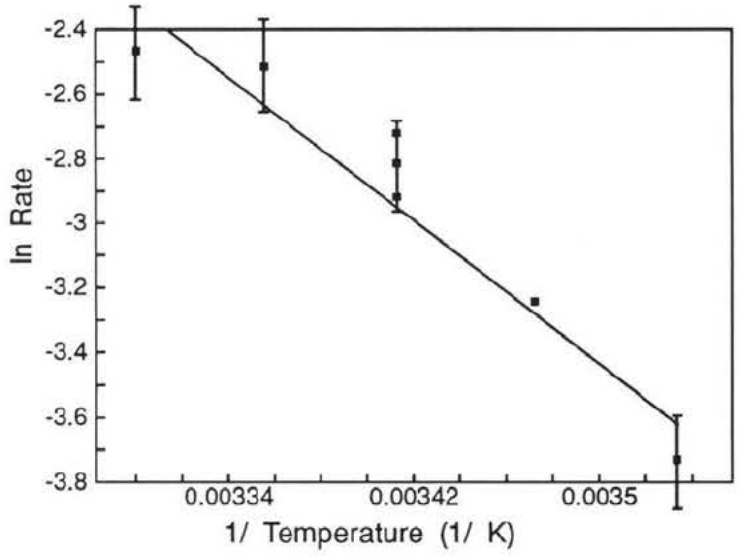

Figure 22 Arrhenius Plot: Valinomycin
- activation energy E_{act} = 46.8 ± 6.6 kJ/mol, r^2 = 0.909.

valinomycin, the mimic's activation energy was more comparable to gramicidin. Following the logic of Eisenman's[36] study, the $(G8TrgP)_6$ mimic is not a carrier.

Transport experiments using dimyristoyl phosphatidylcholine vesicles were attempted, but the vesicles were unstable over the time periods necessary for the study due to an extremely fast rate of leakage.

Cation Selectivity

The cation selectivity study examined the relative rates and extent of transport associated with the alkali earth cations: lithium, sodium, potassium, rubidium, and cesium as sulphate salts (see Table VII, Table VIII, and Table X). The transporter concentrations were used in the saturation range; the cation concentration was 95 mM for the selectivity study on the mimic and valinomycin, 50 mM for gramicidin. Figure 23 shows the experimental data curves for the cations lithium through cesium, in order of increasing rate and extent of transport due to the $(G8TrgP)_6$ mimic.

Table VII

Dependence of k_{obs}, Extent of Transport, and Overall Rate as a Function of Cation: $(G8TrgP)_6$ Mimic

Cation	[a]k_{obs}	Extent of Transport	[b]Rate
	x 10^{-3} s^{-1}	%	x 10^{-2} s^{-1}
Li^+	$10.^7$	4	0.04
Na^+	6.9^0	14	0.10
K^+	6.5^0	27	0.17
Rb^+	7.6^3	31	0.24
[c]Cs^+	7.2^7	41	0.30

a) 25 °C; [$(G8TrgP)_6$ mimic] = 4 x 10^{-7} M; [M^+] = 95 mM; [FCCP] = 0.18 µM; r^2 values for fit to first order regression were >0.998.
b) rate expressed as percent H^+ available transported per second; absolute rate for K^+ (transport volume was 0.090 mL of 4.75 mM choline base) was 28 x 10^{-10} mol $H^+ \cdot s^{-1}$.
c) duplicate run on Cs^+: rate = 0.30 x 10^{-2} s^{-1} ± 4%; therefore, all rates are statistically different, even using a standard deviation value of ±10% for all cations.

Figures 24 and 25 also compare the rates and extents of transport for the mimic and gramicidin. In Figure 24, the extent of transport and the rate are very closely related, suggesting that the rate actually depends upon the extractibility of the cation using whatever mechanism the mimic employs. Figure 26 shows the very discriminating nature of valinomycin in its cation selectivity; different to both the mimic and gramicidin.

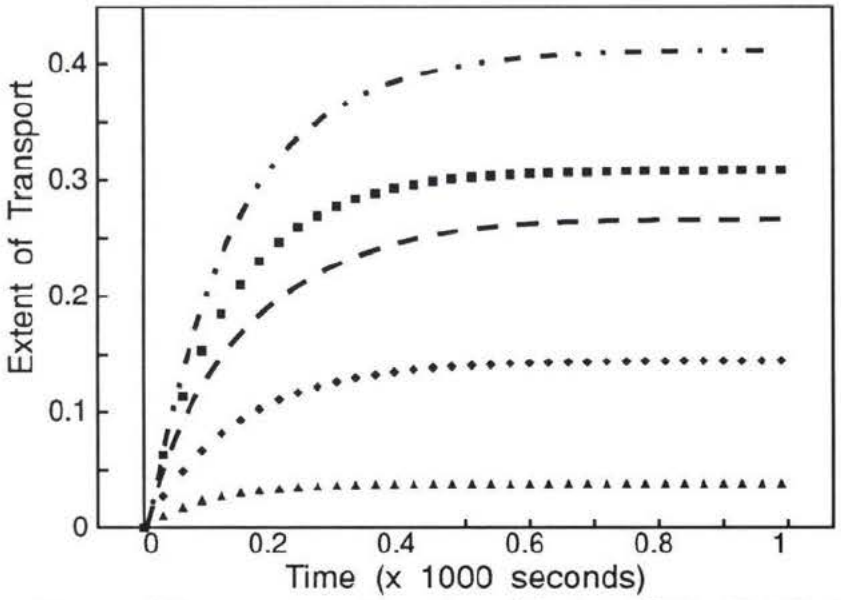

Figure 23 Extent of Transport as a Function of Cation: $(G8TrgP)_6$ Mimic - for cations of Li(▲), Na(♦), K(--), Rb(■), and Cs(···)

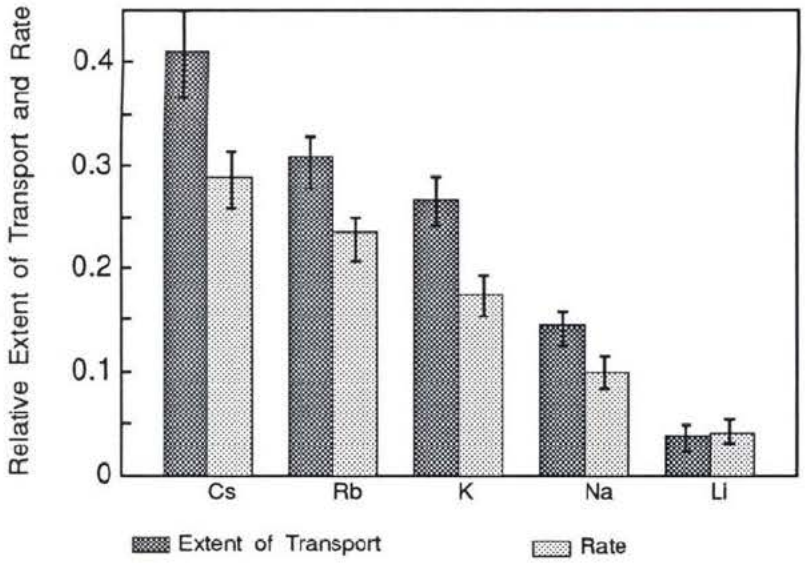

Figure 24 Bar Graph of Rate and Extent of Transport for Alkali Metal Cations: $(G8TrgP)_6$ Mimic

The trend observed for the mimic appears related to the size of the bare cation[30] and/or the ease of dehydration[45] (see Table IX). However, the selectivity sequence does not match that for 18-crown-6[46]; this is reasonable since the crown ether selectivity also depends on the coordinating anion which might not be relevant to a channel mechanism. However, the

Table VIII

Dependence of k_{obs}, Extent of Transport, and Overall Rate as a Function of Cation: Gramicidin

Cation	Cation Conc'n.	[a]k_{obs}	Extent of Transport	[b]Rate
	mM	x 10^{-3} s^{-1}	%	x 10^{-2} s^{-1}
Li^+	54	7.9[7]	53	0.42
Na^+	44	8.9[7]	52	0.47
K^+	51	7.2[0]	53	0.38
Rb^+	50	9.6[0]	52	0.50
Cs^+	50	7.1[0]	52	0.37

a) 20 °C; [gramicidin] = 6.6 x 10^{-9} M; [FCCP] = 0; r^2 values for fit to first order regression were >0.98; no chloroform used.
b) rate expressed as percent H^+ available transported per second; absolute rate for K^+ (transport volume was 0.155 mL of 4.75 mM choline base) was 53 x 10^{-10} mol $H^+ \cdot s^{-1}$.

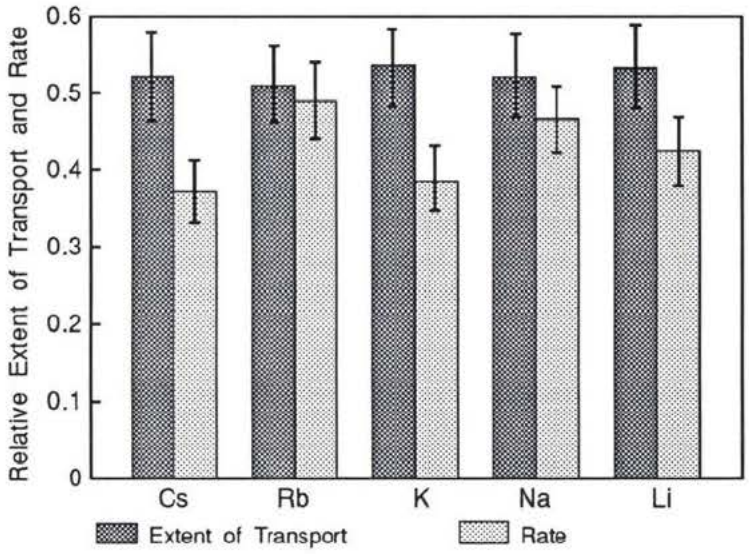

Figure 25 Bar Graph of Rate and Extent of Transport of Alkali Metal Cations: Gramicidin

$(G8TrgP)_6$ mimic cation selectivity also matches the sequence found for gramicidin in erythrocyte lipid/ n-decane black lipid membranes. Gramicidin's selectivity is attributed to a "libration" mechanism, where the diameter of the gramicidin lumen alters to increase the bonding interactions between the bare cation and the inner wall of the lumen to offset the

Table IX
Summary of Cation Properties and Transporter Selectivities

Ion	$(G8TrgP)_6$ Mimic[a]	Ionic Radius	Dehydration Energy	[b]18-C-6	Gramicidin
	percent transport	Å	kJ/mol	log K_s	permeability ratio
Li^+	4	0.68	520	<0.5	0.33
Na^+	14	0.97	405	4.38	1.0
K^+	27	1.33	321	6.20	3.9
Rb^+	31	1.47	300	5.30	5.5
Cs^+	41	1.67	277	4.55	5.8
	[a]Ratio to Na^+				
Li^+	0.3	0.77	0.78	<0.11	0.33
Na^+	1.0	1.00	1.00	1.00	1.0
K^+	1.9	1.48	1.26	1.42	3.9
Rb^+	2.2	1.55	1.35	1.21	5.5
Cs^+	2.9	1.56	1.46	1.04	5.8

a) $(G8TrgP)_6$ mimic selectivity based on protons transported as a percent of protons entrapped; ratios to sodium chosen due to gramicidin data.
b) stability constants for 18-crown-6 as reported in Inoue, for 1:1 complexation of metal perchlorate in methanol/benzene (80/20 v/v) at 25 °C.

dehydration energy as the cation transfers from the aqueous environment to the channel[30]. Hladky and Haydon[47] found a somewhat different selectivity sequence for gramicidin; Rb≥Cs>K>Na>Li.

It is interesting to note that in the "unsoftened" vesicle experiments, gramicidin has no apparent selectivity for these cations. The variances in the extents of transport and the rates fall within experimental error. The selectivity sequence as given in Table IX for gramicidin was determined using BLMs, which are likely to have high fluidity because of the large amount of solvent surrounding the bilayer. Possibly, the libration mechanism can only occur

Table X

Dependence of k_{obs}, Extent of Transport, and Overall Rate as a Function of Cation: Valinomycin

Cation	[a]k_{obs}	Extent of Transport	[b]Rate
	x 10^{-3} s^{-1}	%	x 10^{-2} s^{-1}
Li^+	-	-	
Na^+	-	-	
K^+	2.4[3]	62	0.15
Rb^+	3.1[5]	59	0.19
Cs^+	1.7[5]	65	0.11

a) 25 °C; [M^+] = 95 mM; [FCCP] = 0.15 µM; r^2 values for fit to first order regression >0.99. (- represents no detectible transport event); no chloroform used.
b) rate expressed as percent H^+ available transported per second; absolute rate for Rb^+ (transport volume = 0.243 mL of 3.98 mM choline base) was 30 x 10^{-10} mol $H^+.s^{-1}$.

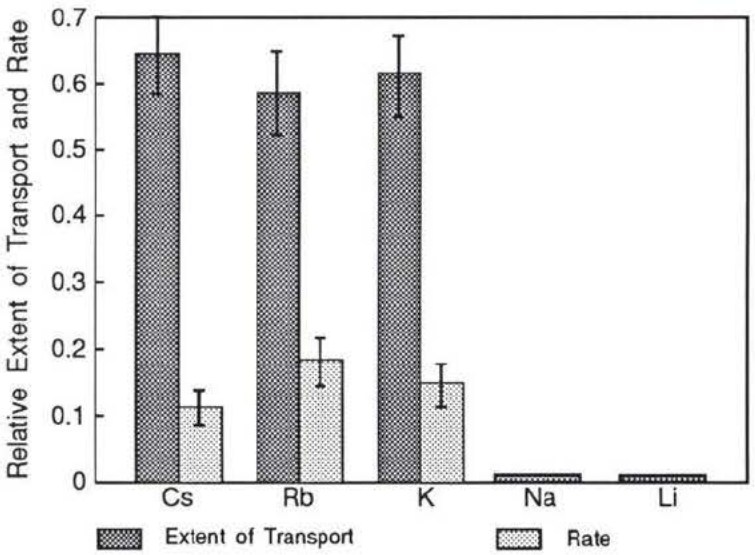

Figure 26 Bar Graph of Rate and Extent of Transport of Alkali Metal Cations: Valinomycin

in very fluid membranes, allowing the structure to expand and contract easily. In that case, the $(G8TrgP)_6$ mimic may also have a different selectivity sequence in "unsoftened" vesicles. Overall, the results give no indication of the mechanism involved in the $(G8TrgP)_6$ mimic transport process. The best comparison of selectivity is to the ease of dehydration of the

cations. This suggests that the cations are not passively diffusing through a water-filled hole formed by some aggregation of mimic molecules, but gaining some benefit from interacting with the mimic. Also, the cations are not passively diffusing through the membrane, as there is a substantial energy barrier, arising from the repulsive interaction between a bare or hydrated ion and the lipid of the membrane. The selectivity sequence for solvation into formamide, N-methyl acetamide and dimethyl formamide[48], is $K^+ > Rb^+ > Cs^+ > Na^+ > Li^+$, noticeably different from the selectivities determined for the transporters in this study.

Cesium and Potassium Concentration Dependence

In order to gain more insight into the mechanism of cation transport via the $(G8TrgP)_6$ mimic, the concentration dependence of two cations was investigated. Cesium was chosen as it was transported the most quickly (see Table XI); potassium was chosen as it was used in all the other experimental series (see Table XII). Comparison of cesium and lithium was not feasible, since the small rate observed for a high concentration of lithium limited the concentration range from which accurate rates could be measured.

Table XI

Dependence of k_{obs}, Extent of Transport, and Overall Rate as a Function of the Concentration of Cesium: $(G8TrgP)_6$ Mimic

Cesium Concentration	[a]k_{obs}	Extent of Transport	[b]Rate
mM	x 10^{-3} s^{-1}	%	x 10^{-2} s^{-1}
0	2.2^5	2	0.01
6	6.1^3	17	0.10
23	6.0^0	36	0.22
44	6.9^5	52	0.36
56	7.8^0	50	0.39
164	$10.^5$	59	0.62
318	$12.^3$	61	0.76
318	$11.^5$	62	0.71
319	$11.^0$	60	0.65

a) 25 °C; [$(G8TrgP)_6$ mimic] = 4 x 10^{-7} M; [FCCP] = 0.18 μM; r^2 values for fit to first order regression were >0.999; standard deviation calculated from triplicate on cesium, ± 8%.
b) rate expressed as percent H^+ available transported per second; absolute rate for [Cs^+] = 164 mM (transport volume was 0.184 mL of 3.98 mM choline base) was 77 x 10^{-10} mol $H^+ \cdot s^{-1}$.

The graph in Figure 27 shows the relationship between rate and concentration of cesium. In order to determine the Michaelis-Menton parameters of V_{max}, maximum rate of transport, and K_m, the concentration of cation to attain half the maximum rate, a Lineweaver-Burk

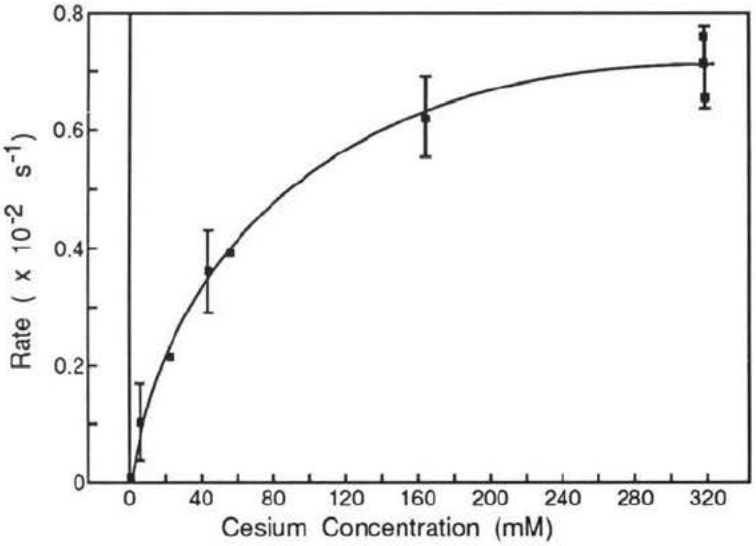

Figure 27 Dependence of Rate as a Function of Cesium Concentration: $(G8TrgP)_6$ Mimic

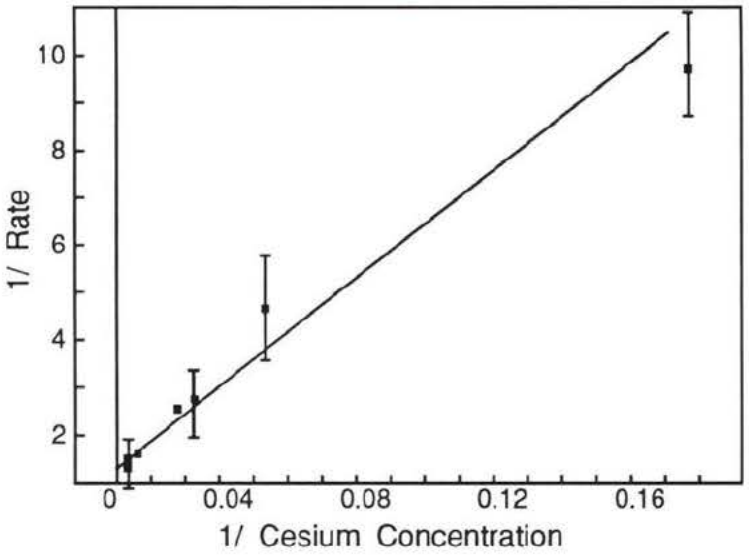

Figure 28 Lineweaver-Burk Plot for Cesium Concentration Dependence of $(G8TrgP)_6$ Mimic

analysis of plotting the inverses of rate against concentration of the cation. The relevant equation is:

$1/rate = 1/[M^+] * (K_m / V_{max}) + 1/V_{max}$. A plot of 1/Rate versus $1/[M^+]$ gives an intercept of $(V_{max})^{-1}$, and a slope multiplied by V_{max} gives K_m. Figure 28 is the Lineweaver-Burk plot of the inverses of rate versus concentration. This plot produced the Michaelis-Menton kinetic

Table XII

Dependence of k_{obs}, Extent of Transport, and Overall Rate as a Function of the Concentration of Potassium: $(G8TrgP)_6$ Mimic

Potassium Concentration	[a]k_{obs}	Extent of Transport	[b]Rate
mM	x 10^{-3} s^{-1}	%	x 10^{-2} s^{-1}
1	8.5[5]	7	0.05
2	7.4[5]	10	0.07
5	5.8[0]	13	0.08
10	6.6[3]	22	0.15
21	7.1[5]	30	0.21
59	5.9[3]	34	0.20
59	5.0[0]	32	0.16
95	7.0[3]	28	0.20
94	6.9[3]	25	0.18
95	5.7[3]	28	0.16

a) 25 °C; [$(G8TrgP)_6$ mimic] = 4 x 10^{-7} M; [FCCP] = 0.18 μM; r^2 values for fit to first order regression were >0.998; triplicate at 95 mM gave standard deviation of ± 10%.
b) rate expressed as percent H^+ available transported per second; absolute rate for [K^+] = 10 mM (transport volume was 0.099 mL of 4.75 mM choline base) was 21 x 10^{-10} mol $H^+ \cdot s^{-1}$.

parameters for cesium: V_{max}, the maximum rate, was 0.66 ± 0.2 x 10^{-2} s^{-1} (this relates to an absolute rate of approximately 72 x 10^{-10}mol $H^+ \cdot s^{-1}$), and K_m, the molarity to achieve half of V_{max}, was 34 ± 2 mM. The saturation concentration range of cesium was above 200 mM; this was twice the concentration used for the selectivity study. The selectivity sequence is, therefore, a conservative estimate, since a higher concentration of cesium, and rubidium, would have increased the discrimination to the other ions.

The Lineweaver-Burk plots for potassium concentration dependence of the mimic, gramicidin, and valinomycin are shown in Figures 29, 30, and 31. Each of the transporters was used within its saturation concentration range. The gramicidin and valinomycin data was acquired using "non-softened" vesicles (see Table XIII and Table XIV). Whether chloroform

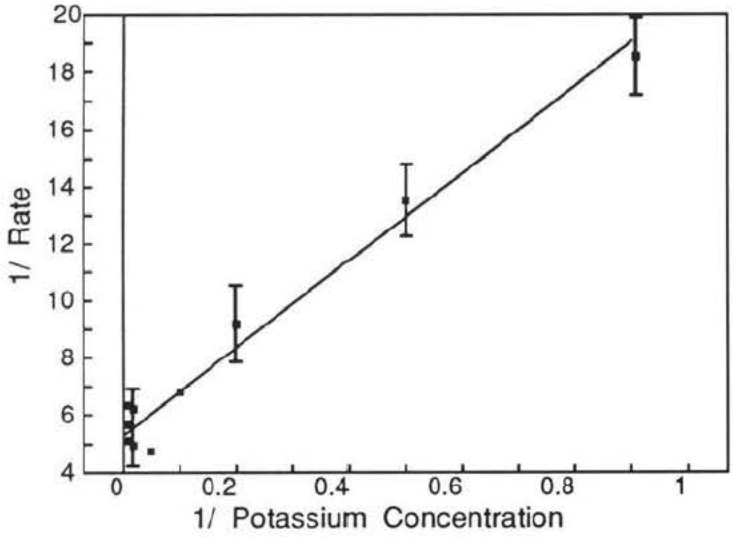

Figure 29 Lineweaver-Burk Plot for Potassium Concentration Dependence of $(G8TrgP)_6$ Mimic

affects their cation concentration dependence was not examined. Comparison of the K_m values to distinguish mechanisms was not valid since the selectivity sequences for the transporters were all different. It was just coincidence that the mimic and gramicidin had low K_m values for potassium relative to valinomycin; cesium might give a different result.

Divalent Cation Transport

The sulphate salts of copper (II), magnesium, and calcium were used in the pH-stat experiments to determine if the $(G8TrgP)_6$ mimic would induce transport of divalent cations. Cupric sulphate was observed to coagulate the vesicle solution. At a high concentration, 90 mM magnesium ions induced a very slow release of protons from the vesicles, just above the detection limit of the experiment. Calcium ions were transported across the bilayer at approximately 0.08×10^{-2} s^{-1}, similar to lithium, but at a level 100 times less concentrated. A complete concentration dependence study was not performed due to the insolubility of calcium sulphate.

Table XIII

Dependence of k_{obs}, Extent of Transport, and Overall Rate as a Function of the Concentration of Potassium: Gramicidin

Potassium Concentration	[a]k_{obs}	Extent of Transport	[b]Rate
mM	x 10^{-3} s^{-1}	%	x 10^{-2} s^{-1}
1.1	3.1^{5}	18	0.06
6.5	3.3^{0}	39	0.13
21.5	5.2^{7}	47	0.25
51.0	6.2^{3}	52	0.33
51.1	5.7^{3}	54	0.31
51.1	5.6^{0}	54	0.30
97.1	5.5^{3}	54	0.30

a) 20 °C; [gramicidin] = 7 x 10^{-9} M; [FCCP] = 0; r^2 values for fit to first order regression were >0.98; triplicate on 51 mM potassium gave standard deviation of ± 4%.
b) rate expressed as percent H^+ available transported per second; absolute rate for [K^+] = 21.5 mM (transport volume was 0.145 mL of 4.75 mM choline base) was 36 x 10^{-10} mol $H^+ s^{-1}$.

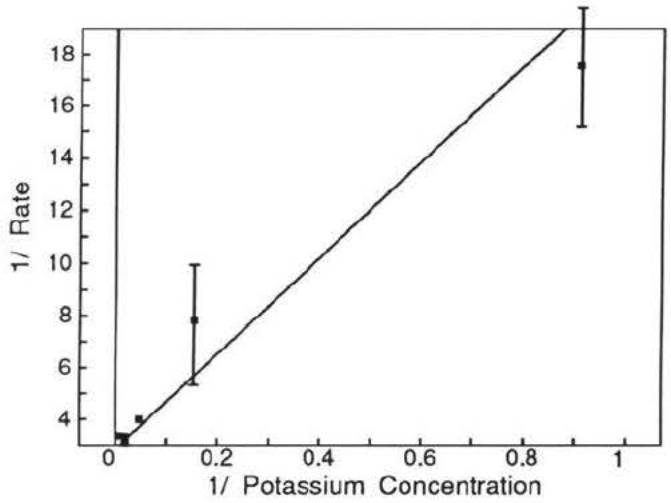

Figure 30 Lineweaver-Burk Plot for Potassium Concentration Dependence of Gramicidin

Table XIV

Dependence of k_{obs}, Extent of Transport, and Overall Rate as a Function of the Concentration of Potassium: Valinomycin

Potassium Concentration	[a]k_{obs}	Extent of Transport	[b]Rate
mM	x 10^{-3} s^{-1}	%	x 10^{-2} s^{-1}
11	1.6[3]	57	0.09
21	2.3[3]	62	0.14
52	3.1[3]	76	0.24
52	3.4[0]	67	0.23
52	3.3[0]	69	0.23
99	4.0[0]	74	0.30
142	4.1[3]	74	0.30
180	3.7[0]	80	0.30

a) 20 °C; [valinomycin] = 6.9 x 10^{-7} M; [FCCP] = 0.16 µM; r^2 values for fit to first order regression were >0.99; triplicate at 52 mM potassium gave standard deviation of ± 3%; no chloroform used.

b) rate expressed as percent H^+ available transported per second; absolute rate for 99 mM (transport volume was 0.210 mL of 4.75 mM choline base) was 40 x 10^{-10} mol $H^+ \cdot s^{-1}$.

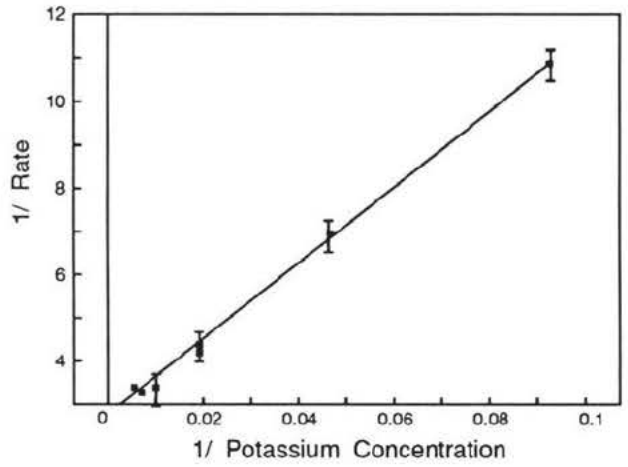

Figure 31 Lineweaver-Burk Plot for Potassium Concentration Dependence of Valinomycin

Inhibition of Potassium Transport

All the previous data supports the idea that the $(G8TrgP)_6$ mimic facilitates the transport of cations through the vesicle membrane. A channel mechanism of transport can be inferred from comparisons to the behaviour of gramicidin and valinomycin. Whether the cations actually move through the center of the mimic cannot be established by any of the previous experiments.

Octylammonium sulphate was added to the pH-stat experiment in place of potassium sulphate, and there was no observed transport. Potassium sulphate was added after several minutes, and still no transport occurred. Gramicidin was then added, and the rate observed was many times lower than expected for the concentrations used. Valinomycin was added, and the subsequent rate was much faster than observed for the gramicidin; apparently it was not affected by the octylammonium cation. The octylammonium cation evidently blocked the transport of potassium by the mimic and gramicidin.

To establish the type of inhibition (non-competitive or competitive) a family of curves needed to be generated to determine the V_{max} and K_m for different concentrations of potassium and octylammonium cations. This study was not attempted since the number of individual runs would require more than one batch of vesicles, and the between batch comparisons were not reliable.

The dependence of the rate of potassium transport on the octylammonium concentration was investigated (see Table XV). As shown in Figure 32, the inhibition was dramatic. At 2 μM concentration of octylammonium, a 10:1 ratio of octylammonium cation to mimic, the rate of transport was negligible. Higher concentrations of the inhibitor did not decrease this rate; lower concentrations, one half and one fifth the mimic concentration, allowed for increasing transport rates. The binding of the alkyl ammonium salts in 18-crown-6 crown ethers is less than potassium[49]. Considering the environment the crown ether framework of the mimic, the solvation of the octylammonium cation is obviously preferred, and apparently strong enough

to prevent transport of the molecule through the orifice of the mimic. This evidence supports the idea that the cation travels through the center of the mimic structure.

Table XV

Dependence of k_{obs}, Extent of Transport, and Overall Rate of Potassium Transport as a Function of the Concentration of Octylammonium Sulphate Inhibitor

Octylammonium Concentration	[a]k_{obs}	Extent of Transport	[b]Rate
x 10^{-6} M	x 10^{-3} s^{-1}	%	x 10^{-2} s^{-1}
0	4.3^3	26	0.11
0.4	4.6^5	14	0.07
0.9	4.0^0	15	0.06
2	3.5^3	4	0.01
5	3.3^5	7	0.02
45	3.2^7	4	0.01

a) 25 °C; [$(G8TrgP)_6$ mimic] = 4 x 10^{-7} M; [K^+] = 41 mM; [FCCP] = 0.15 µM; r^2 values for fit to first order regression were >0.99.
b) rate expressed as percent H^+ available transported per second; absolute rate for no inhibitor (transport volume was 0.131 mL of 3.98 mM choline base) was 23 x 10^{-10} mol H^+s^{-1}.

Has the presence or absence of chloroform had an effect on the outcome of this study? Considering all factors, the chloroform apparently only affected the fluidity of the bilayer membrane. The mimic is capable of inducing transport without chloroform "softening" of the vesicles, but the subsequent rates are very low and unreliable as they are at the bottom of the dynamic range of the pH-stat experiment. With the chloroform added to the vesicles the observed rates increase. It is unlikely that the chloroform is helping the mimic insert into the membrane; recent studies into the mimic's partitioning between the aqueous and lipid volumes show that it is mostly in the bilayer, with or without chloroform present[43]. These "add-back" experiments were performed on the precursor mimic[26] (Dutton), and it was found to partition completely into the vesicle. As mentioned before, other anaesthetics such as ether,

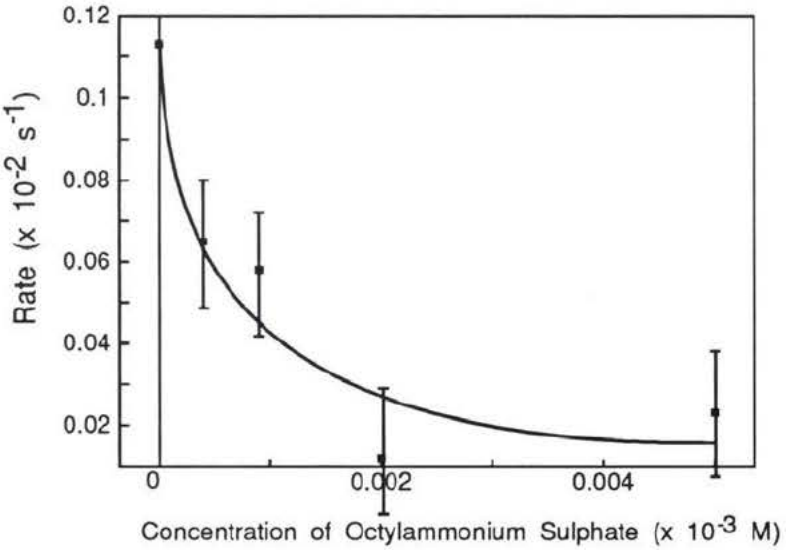

Figure 32 Rate of Potassium Transport versus Concentration of Octylammonium Sulphate for $(G8TrgP)_6$ Mimic

dichloromethane, and halothane worked similarly to chloroform (albeit at different concentrations), but hexane did not. The mimic is very soluble in hexane, and if the faster rates were produced by increased solvation into the membrane then hexane should have worked as well as the others. This indicates that it is the "softening" of vesicles, not the aiding of transporter insertion into the vesicles, which increased the observed transport rates for the mimic. It is possible that the chloroform "softened" vesicles extend the open lifetime of the mimic, allowing more transport to occur per opening, and hence faster observed rates.

Is the $(G8TrgP)_6$ Mimic an Ion Channel?

Yes. Supported by three lines of evidence: The first and most complete line of evidence is my data, fully summarized below.

The second line of evidence comes from the pipette-dipping experiments using the Dutton mimic, performed by Dr. M. Sansom. The results gave unequivocal evidence of channel formation. Figure 33 shows unit conductance in current as a function of time. The bilayer composition was diphytanoyl phosphatidylcholine and n-pentane. Analysis of the data of Figure 33 suggested three independently acting channels.

The third line of evidence is derived from a structure activity study completed by James as part of his doctoral research[43]. One of his conclusions is that minor variations in length, such as the difference between the Dutton and James mimics, might alter the absolute rate, but would not alter the mode of action of the mimics. In no case does such a minor variation in structure shift the mode of action from channel to carrier. It is therefore likely that the $(G8TrgP)_6$ mimic in Sansom's experiment would be an ion channel.

The first conclusion that can be drawn from my own experimental work is that the $(G8TrgP)_6$ mimic is definitely a transporter. It is not a detergent because a cation gradient was required to induce the release of protons from the vesicles. It does not create membrane defects since there is a cation selectivity which is different from the sequence found for the extraction of the ions from water into lipid. It does not aggregate to form large water filled holes since FCCP is required to collapse the proton gradient in response to the movement of cations across the membrane. Either the mimic is a carrier and complexes with the cations and diffuses across the membrane, releasing them once across, or it is a channel and provides a hole through which the cations may travel to the other side of the bilayer.

The results obtained from the many series of experiments do not absolutely establish the mechanism by which the $(G8TrgP)_6$ mimic works. As was mentioned before, it is simple to visualize the difference between carriers and channel, but merely observing the translocation

of ions across a membrane does not determine the mechanism employed. The transporter mechanism of the $(G8TrgP)_6$ mimic was inferred from pairwise comparison with gramicidin and valinomycin with respect to transporter concentration dependence, temperature dependence, cation selectivity and concentration dependence, inhibitor concentration dependence, and ion conductivity response. Gramicidin and valinomycin have channel and carrier mechanisms, respectively. They were chosen as models of their transporter classes due to the simplicity of their structures and the amount of research already performed to characterize their behaviours, both in black lipid membranes and in vesicles.

In comparison to valinomycin, the mimic had a similar implied kinetic order as established by the log-log plot of rate versus concentration. However, all three of the transporters had similar kinetic orders, thus the results are equivocal. The cation selectivities of valinomycin and the mimic were different, but that is not an indication of mechanism, merely characteristic of the transporters' structures. The Michaelis-Menton parameters were also different for the potassium concentration dependence; again, that is not a mechanistic factor.

With respect to the factors which do indicate mechanism, in comparison to valinomycin the mimic exhibits three distinctive differences. Valinomycin has a constant extent of transport independent of its concentration, which suggests that it induces transport in the vesicles into which it initially partitions and then moves on to function in other vesicles. The $(G8TrgP)_6$ mimic produces extents of transport which are definitely concentration dependent, thus implying that the mimic only acts in, and remains within, the vesicle into which it partitions. Valinomycin has an activation energy much greater than that of the mimic. The mimic's negligible activation energy indicates that the extraction of the cations from the aqueous into the lipid volume is not a rate determining step; whereas, the extraction of the cations by valinomycin is made easier with an increase in temperature. The most marked difference in this pairwise comparison was the inhibition of the mimic, and not valinomycin, by the octylammonium cation. It is difficult to envision how a carrier could be inhibited by

complexation; no such examples are known[9,10].

In comparison to gramicidin the differences to the mimic's behaviour are insignificant with respect to the determination of a transporter mechanism. The cation selectivity difference has already been mentioned, and it is due only to the differences of shape and structure of the two transporters. The only other dissimilarity lies in the concentration of transporter required to induce the translocation of the cations across the membrane. This is easily attributed to the greater activity of gramicidin, which does not preclude the mimic from having a channel mechanism. One likely possibility is that the lifetime of the open state of gramicidin is much longer than the mimic's, possibly long enough to empty an entire vesicle in one opening event whereas the mimic may require many opening events to collapse the gradients across a vesicle wall. Obviously, the differences between gramicidin and the mimic are insignificant with respect to their similarities: low activation energies, extent of transport dependence on concentration, and inhibition by the octylammonium cation - all of which are consistent with a channel mechanism.

Thus, in a vesicle system, the $(G8TrgP)_6$ mimic has critical dissimilarities to the action of valinomycin, and insignificant differences compared to gramicidin. There are no similarities to valinomycin that could sustain an argument that the mimic acts with a carrier mechanism. The experiments produced strong evidence in support of the mimic's being analogous to gramicidin. Therefore based on the fact that the mimic does act as a transporter and that its behaviour closely imitates gramicidin, the conclusion is that the $(G8TrgP)_6$ mimic acts as an ion channel.

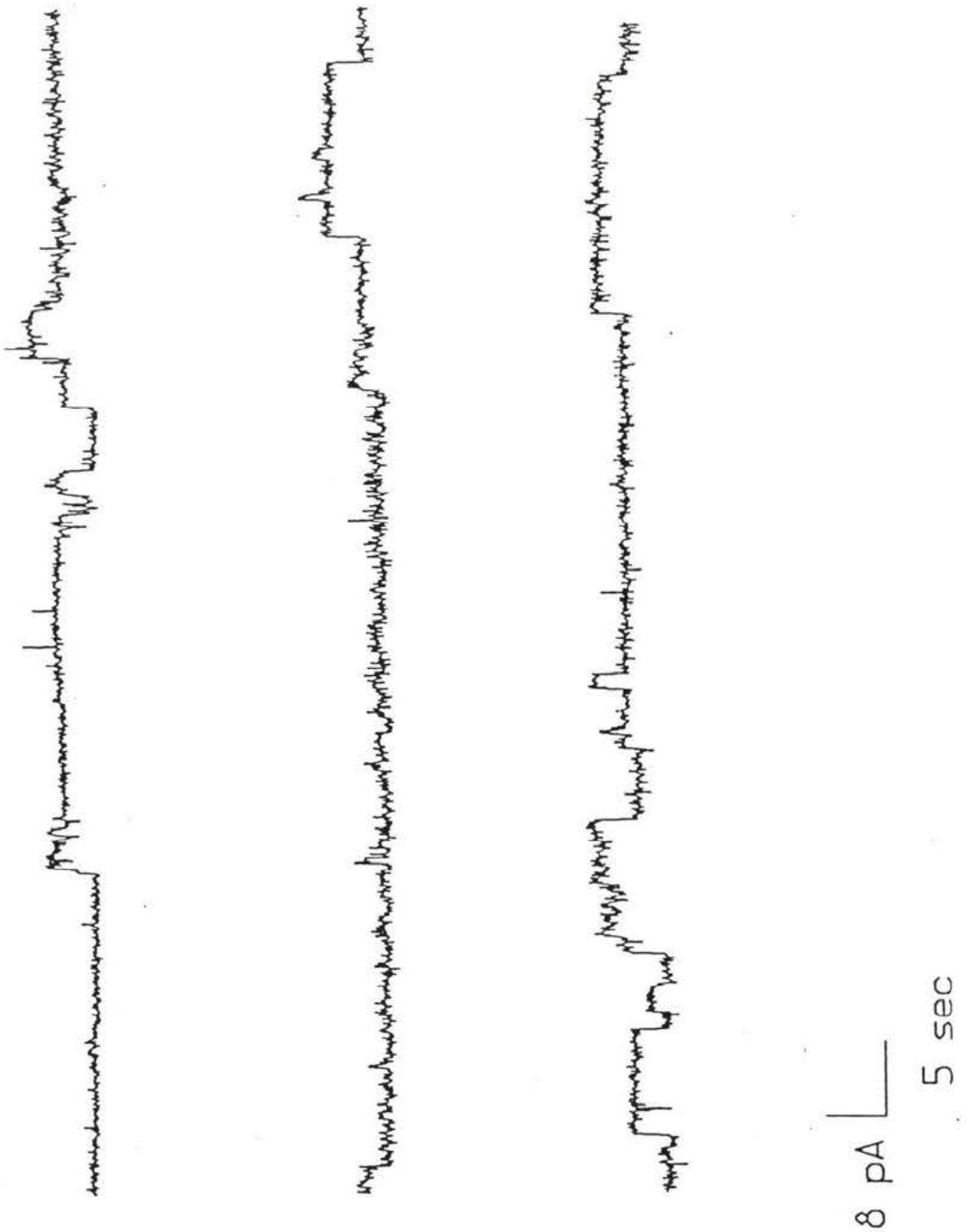

Figure 33 Conductivity versus Time of the Mimic synthesized by Dutton - experiment performed by Dr. M. Sansom.

REFERENCES

1. P.C. Jordan, *J. Phys. Chem.*, **91**, 6582 (1987).

2. M. Hervé, B. Cybulska, C.M. Gary-Bobo, *European Biophysics Journal*, **12**, 121 (1985).

3. F.G. Riddell, S. Arumugam, A.Patel, *Inorg. Chem.*, **29**,2398 (1990).

4. F.G. Riddell, S. Arumugam, B.G. Cox, *J. Chem. Soc., Chem. Commun.*, 1890 (1987).

5. R.N. Robertson, "The Lively Membranes", Cambridge University Press 1983, Cambridge p.128.

6. G.R. Painter, B.C. Pressman, *Topics in Current Chemistry*, vol.128 pp.83 - 110.

7. S. Kimura, Y. Imanishi, "Peptide Chemistry 1985", ed. Y. Kiso, Protein Research Foundation, Osaka (1986), p.273.

8. TC. Wun, R. Bittman, *Biochem.*, **16**, 2020 (1977).

9. T.M. Fyles, *Frontiers in Bioorganic Chemistry*, **1**, 71 (1990).

10. H. Tsukube, "Liquid Membranes: Chemical Applications, (ed.) T. Araki and H. Tsukube, CRC Press, Inc., Boca Raton, Florida, 1990. pp. 51-75.

11. R.C. Warren, "Physics and the Architecture of Cell Membranes", IOP Publishing Ltd., Bristol, England, 1987, pp.40 - 42.

12. N. Unwin, *Chemica Scripta*, **27B**, 47 (1987).

13. H. Betz, *Biochem.*, **29**, 3591 (1990).

14. G.A. Woolley, C.M. Deber, *Biopolymers*, **28**, 267 (1989).

15. M. Bhakoo, T.H. Birkbeck, J.H. Freer, *Can. J. Biochem. Cell Biol.*, **63**, 1 (1985).

16. A.W. Bernheimer, B. Rudy, *Biochim. Biophys. Acta*, **864**, 123 (1986).

17. P. De Santis, A. Palleschi, M. Savino, A. Scipioni. B. Sesta, A. Verdini, *Biophys. Chem.*, **21**, 211 (1985).

18. K. Kono, S. Kimura, Y. Imanishi, *J. of Membr. Science*,**58**, 1 (1991).

19. G. Spach, Y. Merle, G. Molle, *Journal de Chimie Physique*, **82**, 719 (1985).

20. A. Pullman, *Pure & Appl. Chem.*, **60**, 259 (1988).

21. I. Tabushi, Y. Kuroda, K. Yokota, *Tet. Lett.*, **23**, 4601 (1982).

22. A. Nakano, Q. Xie, J.V. Mallen, L. Echegoyen, G.W. Gokel, *J. Am. Chem. Soc.*, **112**, 1287 (1990).

23. F.M. Menger, D.S. Davis, R.A. Persichetti, J.-J. Lee, *J. Am. Chem. Soc.*, **112**, 2451 (1990).

24. R.J.M. Nolte, A.J.M. van Beunen, J.G. Neevel, J.W. Zwikker, A.J. Verkley, W. Drenth, *Isr. J. Chem.*, **24**, 297 (1984).

25. V.E. Carmichael, P.J. Dutton, T.M. Fyles, T.D. James, J.A. Swan, M. Zojaji, *J. Am. Chem. Soc.*, **111**, 767 (1989).

26. T.M. Fyles, T.D. James, K.C. Kaye, *Can. J. Chem.*, **68**, 976 (1989).

27. J.-M. Lehn, P.G. Potvin, *Can. J. Chem.*, **66**, 195 (1988). L. Julien, J.-M. Lehn, *Tetrahedron Lett.*, **29**, 3803 (1988).

28. O.S. Andersen, *Ann. Rev. Physiol.*, **46**, 531 (1984).

29. B.A. Wallace, K. Ravikumar, *Science*, **241**, 182 (1988).

30. D.W. Urry, *Topics in Current Chemistry*, Vol. 128, 1985, pp. 175-218.

31. C. Miller, *Gen. Physiol.*, **79**, 869 (1982).

32. M. Castaing, F. Morel, J.-M. Lehn, *J. Membrane Biol.*, **89**, 251 (1986).

33. M. Ueno, T. Yasui, I. Horikoshi, *Bull. Chem. Soc. Jpn.*, **56**, 1652 (1983).

34. L. Louni, J.L. Rigaud, C.M. Gary-Bobo, (ed) G. Spach, "Physical Chemistry of Transmembrane Ion Motions", Elsevier Sci. Publ., Amsterdam, Oxford, New York, pp. 319-326 (1983).

35. I.R. Mellor, M.S.P. Sansom, *Proc. R. Soc. Lond.*, B **239**, 383 (1990).

36. S. Krasne, G. Eisenman, G. Szabo, *Science*, **174**, 412 (1971).

37. J. Fendler, "Membrane Mimetic Chemistry", John Wiley & Sons, Inc., NY. (1982), p.127.

38. R.R.C. New "Liposomes - a practical approach", IRL Press, Oxford University Press New York 1990 pp. 33 - 103.

39. F. Szoka, F. Olson, T. Heath, W. Vail, E. Mayhew, D. Papahadjopoulos, *Biochim. Biophys. Acta*, **601**, 559 (1980).

40. J.H. Lakey, M. Ptak, *Biochem.*, **27**, 4639 (1988).

41. P.J. Dutton, *Doctoral Dissertation*, University of Victoria, Victoria B.C., Canada, 1988. p.236.

42. J.-M. Camaleño-Delgado, X.K. Zhao, J.H. Fendler, *Can. J. Chem.*, **68**, 888 (1990).

43. T.D. James, private communication, work in progress.

44. S. Mabrey, P.L. Mateo, J.M. Sturtevant, *Biochem.*, **17**, 2464 (1978).

45. P. Atkins, "Physical Chemistry", 2nd edition, Oxford University Press, Great Britain (1982) p.123.

46. Y. Inoue, G.W. Gokel (eds.) " Cation Binding in Macrocycles", Marcel Dekker, Inc., NY. (1990), p.535.

47. S.B. Hladky, D.A. Haydon, *Biochim. Biophys. Acta*, **274**, 294 (1972).

48. S. Krasne, G. Eisenman, "Membranes, Lipid Bilayer and Antibiotics", Vol.2, ed. G. Eisenman. Marcel Dekker, Inc., New York. 1973, p.273.

49. R.M. Izatt, J.S. Bradshaw, S.A. Nielsen, J.D. Lamb, J.J. Christensen, D. Sen, *Chem. Rev.*, **85**, 271 (1985); and references therein.

VITA

KAYE, Katharine Clare

Born May 4,1964, Victoria, B.C., Canada

Educational Institutions Attended:

University of Victoria 1983 to 1991

Degrees Awarded:

B.Sc. (Honours) University of Victoria 1988

Publications and Presentations:

T.M. Fyles, T.D. James, K.C. Kaye, "Biomimetic Ion Transport: On the Mechanism of Ion Transport by an Artificial Ion Channel Mimic", *Can. J. Chem.*, **68**, 976 (1990).

T.M. Fyles, K.C. Kaye, T.D. James, D.W.M. Smiley, "Biomimetic Ion Transport: Synthesis and Activity of an Amphotericin Mimic", *Tetrahedron Lett.*, **31**, 1233 (1990).

B. Dietrich, T.M. Fyles, M.W. Hosseini, J.-M. Lehn, K.C. Kaye, "Proton Coupled Membrane Transport of Anions Mediated by Cryptate Carriers", *J. Chem. Soc., Chem. Commun.*, 691 (1988).

T.M. Fyles, T.D. James, K.C. Kaye, M.S.P. Sansom, "Mechanism of Transmembrane Ion Transport by a Synthetic Ion Channel Mimic", 73rd Canadian Chemical Conference and Exhibition, Dalhousie University, Halifax, N.S., July 15-20, 1990.

T.M. Fyles, T.D. James, K.C. Kaye, M. Zojaji, "Functional Unimolecular Ion Channels", 72nd Canadian Chemical Conference and Exhibition, University of Victoria, Victoria, B.C., June 4-8, 1989.

T.M. Fyles, K.C. Kaye, "Anion Inclusion Complexation: Study of Monoanion Transport Across Artificial Membranes", Chemunications '88, Simon Fraser University, Vancouver, B.C., May 5-7, 1988.

PARTIAL COPYRIGHT LICENSE

I hereby grant the right to lend my thesis to users of the University of Victoria Library, and to make single copies only for such users or in response to a request from the Library of any other university, or similar institution, on its behalf or for one of its users. I further agree that permission for extensive copying of this thesis for scholarly purposes may be granted by me or a member of the University designated by me. It is understood that copying or publication of this thesis for financial gain shall not be allowed without my permission.

Title of Thesis: On the Mechanism of Action of an Ion Channel Mimic

Author: [redacted]

KATHARINE CLARE KAYE

September 19/91

DATE